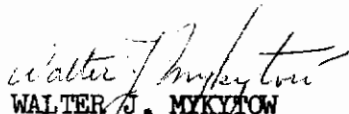# FOREWORD

This report was prepared by the Measurement Analysis Corporation, Los Angeles, California, for the Aero-Acoustics Branch, Vehicle Dynamics Division, AF Flight Dynamics Laboratory, Wright-Patterson Air Force Base, Ohio, under Contract AF33(615)-1314. The study covers transducers for sonic fatigue measurement in connection with optimum utilization of the Sonic Fatigue Facility Data Analysis System. This research is part of a continuing effort to obtain significant information on sound environment simulation and dynamic response to acoustic excitation under the Research & Technology Division, Air Force Systems Command's exploratory development program. The Project No. is 4437, "High Intensity Sound Environment Simulation" and Task No. 443706, "Advanced Instrumentation Study for Sonic Fatigue Experimental Work." Mr. W. K. Shilling, III was the Project Engineer.

The author gratefully expresses his appreciation for the assistance given by O. F. Maurer, J. McCarthy, W. K. Shilling, III, and R. van der Heyde of the Aero-Acoustics Branch of the AF Flight Dynamics Laboratory, and by J. S. Bendat, L. D. Enochson, A. G. Piersol and G. P. Thrall of the Measurement Analysis Corporation.

This technical report has been reviewed and is approved.

WALTER J. MYKYTOW
Asst. for Research & Technology
Vehicle Dynamics Division
AF Flight Dynamics Laboratory

ABSTRACT

This report discusses the machine errors of transducer systems used for the measurement of dynamic input and response data during sonic fatigue testing. The specific types of transducers covered are accelerometers, microphones, and strain gages. The basic operating principles, intrinsic inaccuracies, environmentally related inaccuracies, and usage inaccuracies are described. These inaccuracies are broken down into errors occurring in the transducer, cabling, and signal conditioner, as well as those due to system operation. In addition, methods for minimizing these errors are given.

CONTENTS

CONTENTS (CONTINUED)

LIST OF FIGURES

LIST OF SYMBOLS

A	gain
c	velocity of propagation in inches per second
C	capacitance in farads
C_a	internal capacitance of a piezoelectric transducer in farads
C_c	shunt capacitance of a coaxial cable between a piezoelectric transducer and its signal conditioner in farads
C_i	shunt capacitance of the impedance converter input in farads
e	rms voltage
e_1	output of a transducer in volts rms
e_2	input to a signal conditioner in volts rms
e(t)	instantaneous voltage
$e_1(t)$	instantaneous voltage output of a transducer
$e_2(t)$	instantaneous voltage on the input to a signal conditioner
$e_3(t)$	instantaneous voltage on the output of a signal conditioner
$e_m(t)$	instantaneous voltage developed due to the magnetostrictive effect
e_B	DC excitation voltage
e_D	the DC drift or bias voltage on the output of a signal conditioner
e_N	the noise on the output of a signal conditioner in volts rms
f	frequency in cps
f_n	undamped natural frequency in cps
F	force in rms pounds
F_1	the equivalent force applied to the mass of the microphone in rms pounds
G	conductance in mhos
H(f)	frequency response functions
i	current in rms amperes
I_T	total excitation current required by a Wheatstone bridge under balance conditions in DC amperes
j	$\sqrt{-1}$

k	spring constant in pounds per inch
K	constants
l	length
l_1	the unstrained length of a strain gage (or test specimen length under the strain gage) in inches
Δl	change in length in inches
L	inductance in henries
m	mass in pounds
%N	the hysteresis of a strain gage expressed in percent of full scale
p	sound pressure in rms pounds per square inch
p(t)	instantaneous sound pressure in psi
P	the sound pressure at a specific location in rms psi
q	charge in rms coulombs
R	resistance in ohms
R_a	piezoelectric transducer shunt resistance in ohms
R_i	input resistance of the signal conditioner
$R_g(t)$	the instantaneous resistance of a strain gage in ohms
R_{g_1}	the unstrained resistance of a strain gage in ohms
ΔR_g	the change in resistance of a strain gage in ohms
s	sensitive area of a microphone in square inches
S_1	charge sensitivity of a piezoelectric transducer in rms coulombs per (rms g's, rms psi, etc.)
S_2	voltage sensitivity of a piezoelectric transducer in rms volts per (rms g's, rms psi, etc.)
S/N	signal-to-noise ratio
T	temperature in $^\circ$F
$\ddot{x}$	acceleration in g's rms
X	reactance in ohms
X_C	capacitive reactance in ohms
X_L	inductive reactance in ohms

$y(t)$	instantaneous displacement in inches
Z	electrical impedance in ohms
α	the temperature coefficient of resistance in ohms/ohm per $^{\circ}F$
β	the thermal coefficient of expansion in inches/inch per $^{\circ}F$
ϵ	unit deformation (unit strain)
ϵ_a	apparent strain
ϵ_0	the strain at the midpoint of a strain gage
ϵ_T	the strain transverse to the sensitive axis of a strain gage
$\bar{\epsilon}$	the mean strain over the length of a strain gage
$\epsilon(t)$	the instantaneous strain
ζ	the damping ratio
θ	the angle between the sensitive axis of a transducer and the direction of the parameter being measured in degrees
λ	propagation wave length in inches/cycle
μ	Poisson's ratio
ξ	percent transverse response of a strain gage
τ	time delay in seconds
$\phi(f)$	phase factors

1. INTRODUCTION

To optimize the utilization of the Sonic Fatigue Facility from the viewpoints of (1) the economy of data collection, reduction, and analysis, (2) the elapsed time interval between state of data taking and completion of data analysis, and (3) the absolute accuracy with which measurements are made, it is mandatory that individual contributions of each potential error source be known. The purpose of this report is to evaluate the portion of the total measurement error that can be attributed to the "machine errors"[*] of the transducer systems used during sonic fatigue testing at RTD.

Future reports will discuss the machine errors involved in the recording, editing, and analyzing processes as well as the statistical errors involved in the transducing, recording, editing, and analyzing of random data. It will be a goal of these reports to provide guidelines to assist in the logical, and optimal, distribution of all of the error tolerances. A secondary benefit that will be derived from identifying each individual error source is that of knowing where to concentrate future improvement efforts if higher accuracy measurements become necessary.

The transducer systems discussed in this report have been limited to practical modern systems used for the measurement of oscillatory acceleration, strain, and sound since these are the primary environmental parameters that are measured during sonic fatigue testing. Transducers for the measurement of electrical performance parameters of "black boxes" and static environmental parameters such as temperature, barometric pressure, relative humidity, etc. are considered beyond the scope of this report.

---

[*] "Machine errors" will be defined as the errors in the measurement of any function that can be attributed to imperfections in the equipment, or calibration of the equipment, used to perform the measurement. This is contrasted to "human errors" - errors in reading or interpreting the measurements and to "statistical errors" - errors due to measuring only finite samples of random processes.

1

The machine errors of each type of transducer system have been separated into three categories - intrinsic, environmental, and usage errors. Under intrinsic errors, items such as amplitude response and frequency response are discussed. These are the transducing errors that would still exist even if the usage and environmental errors of the transducing systems could be eliminated. The discussion of environmental errors, the inaccuracies caused by the exposure of the transducers to environments other than those that they were designed to measure, have been limited to the significant environments and environmental ranges that might be reasonably expected in the Sonic Fatigue Test Facility. Such things as transducer calibration, mounting, etc., are discussed under usage errors. Where practical, guidelines for minimizing these errors are given. Emphasis will be placed on discussion of those errors that are the most important. However, all errors will be discussed because an error factor that may be trivial for most measurements may be the most important factor for some particular test.

Selection of the proper category of transducing systems is not discussed in detail because this is not as difficult for laboratory as for field measurements. (The physical restrictions are usually less severe; one usually knows more about the environments, and the measurements can usually be more easily repeated.) However, care should be exercised in the selection of the proper transducers during the pre-test planning if optimal use is to be made of the Sonic Fatigue Facility. The major trade-off that will normally have to be made will be the choice between installing a strain gage or an accelerometer at a particular location. For most cases the choice will be obvious - a strain gage for strain measurements and an accelerometer for vibration measurements. For those cases where it is not, the following guidelines can be used:

2

Where low frequency measurements are of prime importance, use the strain gage system, and conversely, where high frequency measurements are of prime importance, use the accelerometer system.

The rationale behind the above guideline is - the output of a strain gage is proportional to displacement; hence, accurate displacement measurements may be made at low frequencies at acceleration levels too low for direct measurements. Conversely, accurate acceleration levels can be measured at high frequencies where the displacement levels are too low for direct measurement. Although they are not discussed in this report, some consideration should be given to the measurement of displacement (other than strain measurements), velocity, and structural impedance through direct transduction or through the mathematical manipulation of other parameters.

2. ACCELERATION MEASURING SYSTEMS

Many kinds of accelerometers and signal conditioners are presently used for the measurement of dynamic acceleration. Some of the common types, along with their major advantages and disadvantages, are listed in Table 1. At the present time there is no one accelerometer that is ideal for vibration response measurements during acoustic testing. The major goals in the development of such an accelerometer are a very high upper frequency cutoff, a relatively high output sensitivity, small size and weight, and insensitivity to acoustic excitation. The most common type of accelerometer used for the measurement of vibratory response of structures subjected to acoustic excitation are the piezoelectric accelerometers. Generally speaking, the microminiature piezoelectric accelerometers are a good choice. Their major limitations are a lower than desired output sensitivity and a spurious response to acoustic excitation. Since piezoelectric accelerometers will be used at the Sonic Fatigue Facility, the rest of the discussions in this section will be limited to this class of accelerometers.

Because these accelerometers have a source impedance that is primarily capacitive, their signal conditioners are usually either very high input impedance voltage amplifiers or charge amplifiers. Very fine high input impedance voltage amplifiers in both tube and transistorized designs have been readily available for a number of years. These voltage amplifiers do have one inherent disadvantage. The sensitivity of the accelerometer is reduced by both the shunt capacitance occurring in the cabling between the accelerometer and amplifier, and by the input capacitance of the amplifier. Since the RTD Sonic Fatigue Facility is designed with voltage amplifiers, it is important to understand this source of error, and to consider the possible improvement with charge amplifiers.

4

Table 1. Comparison of Accelerometers for Vibration Measurements

Operating Principle	Type Signal Conditioner	Major Advantages	Major Disadvantages
1. Piezoelectric	----	1. Small size and weight 2. Self generating 3. No phase shift over normal operating range	1. High output impedance 2. Cannot be used for DC measurements
	Voltage Amplifier (or Cathode Follower)	1. Good low frequency response	1. Sensitivity is reduced by shunt capacitance between the accelerometer and the signal conditioner 2. High input impedance is required
	Charge Amplifier	1. Sensitivity is not affected by shunt capacity between the accelerometer and the signal conditioner (up to some practical limit)	1. Greater internal noise than voltage amplifiers
2. Unbonded Wire Strain Gage	----	1. DC response 2. Low impedance	1. Phase shift 2. Upper frequency response is proportional to acceleration range 3. Excitation required
	Wheatstone Bridge (DC Excitation)	1. Output is insensitive to reactive unbalance 2. Upper frequency response not limited by excitation voltage	1. A highly stable DC amplifier is required to amplify the low output voltage 2. Floating excitation or amplifier required 3. Highly stable excitation required

Table 1. Comparison of Accelerometers for Vibration Measurements (Continued)

Operating Principle	Type Signal Conditioner	Major Advantages	Major Disadvantages
2. Unbonded Wire Strain Gage (Cont'd)	Wheatstone Bridge (AC Excitation)	1. AC amplification of the bridge output voltage is possible	1. Sensitive to reactive unbalance in the accelerometer and cable to it 2. Floating excitation or amplifier required 3. Highly stable excitation required 4. Upper frequency limited by excitation frequency
3. Piezo-resistance	----	All comments the same as for Item 2 except that this unit has a high output voltage; hence, does not require as much amplification.	
4. Variable Capacitance	----	1. Small size and weight 2. Excellent frequency response	1. Excitation is required 2. High output impedance
	Voltage Divider (DC Excitation)	1. Upper frequency response is not limited by the excitation voltage. 2. No demodulation required	1. High value of excitation voltage is required 2. Sensitivity is reduced by shunt capacitance between the accelerometer and the signal conditioner
	Voltage Divider (AC Excitation)	1. Can obtain DC response	1. Highly stable excitation required 2. Radiation of carrier frequency
4. Variable Inductance	AC Bridge	1. Low impedance 2. DC response	1. Limited frequency range 2. Excitation is required

2.1 VOLTAGE AMPLIFIERS

To illustrate how shunt capacitance decreases the sensitivity of the piezoelectric accelerometer/voltage amplifier combination, consider the simplified equivalent circuits for a piezoelectric accelerometer with an open output, and for this same accelerometer connected to a voltage amplifier through a cable as shown in Figure 1a and Figure 1b, respectively.
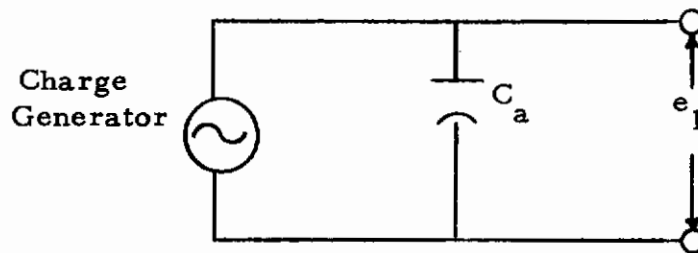
Figure 1a. Simplified Charge Generator Equivalent Circuit of a Piezoelectric Accelerometer
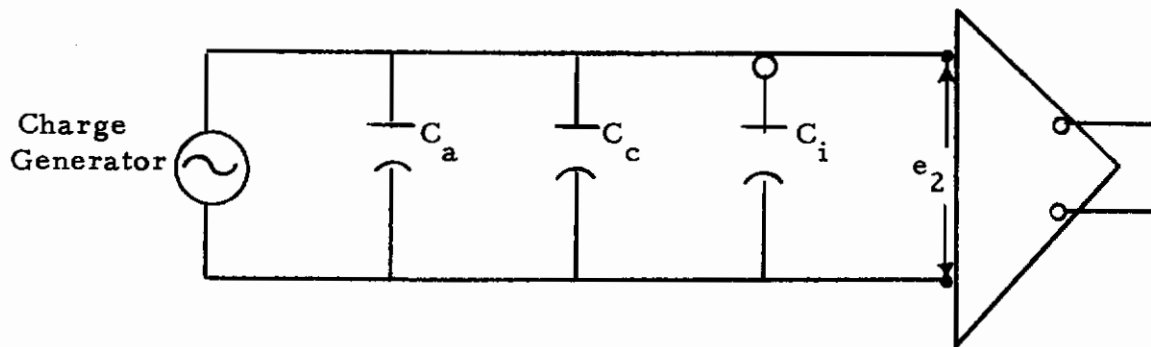
Figure 1b. Equivalent Circuit of a Piezoelectric Accelerometer Connected to a Voltage Amplifier

7

Since the accelerometer generates a charge proportional to the applied acceleration,

$$q = \ddot{x}S_1 \tag{1}$$

For the open circuit case in Figure 1a, the output voltage is

$$e_1 = \frac{q}{C_a} = \frac{\ddot{x}S_1}{C_a} \tag{2}$$

For the actual case, as represented in Figure 1b, where the accelerometer output is connected to shunt capacitance in both the cabling and the amplifier input, the output voltage is

$$e_2 = \frac{q}{C_a + C_c + C_i} = \frac{\ddot{x}S_1}{C_a + C_c + C_i} \tag{3}$$

where

$\ddot{x}$ = applied acceleration in g's rms

S_1 = accelerometer charge sensitivity in coulombs rms/g's rms

e_1 = accelerometer open circuit output in volts rms

e_2 = input to voltage amplifier in volts rms

C_a = internal capacitance of the accelerometer in farads

C_c = shunt capacitance of the accelerometer to voltage amplifier cable in farads

C_i = shunt capacitance of the voltage amplifier input in farads

q = charge in rms coulombs

8

$$e_2 = \left(\frac{\dfrac{\ddot{x} S_1}{C_a + C_c + C_i}}{\dfrac{\ddot{x} S_1}{C_a}} \right) (e_1) = \left(\frac{C_a}{C_a + C_c + C_i} \right)(e_1) \qquad (4)$$

Typical values for the above capacities are:

$$C_a = 500 \times 10^{-12} \text{ farads}$$

$$C_c = 30 \times 10^{-12} \text{ farads/foot of cable}$$

$$C_i = 25 \times 10^{-12} \text{ farads}$$

Hence, where long cables between the accelerometer and signal conditioner are necessary, as in the Sonic Fatigue Facility, the sensitivity of the accelerometer system is sharply reduced. For example, 16 feet of cabling reduces the sensitivity fifty percent. This becomes an even more serious problem when microminiature accelerometers are used since their internal capacitance (C_a) and charge sensitivity (S_1) are lower than those of standard accelerometers. The other disadvantage of voltage amplifiers is that either an in-place calibration must be made, or the shunt capacitance of all cables and signal conditioners must be measured to determine the actual sensitivity of the accelerometer system.

2.2 CHARGE AMPLIFIERS

Charge amplifiers are not subject to the above problems because their output voltage is proportional to their input charge. Hence, shunt capacitance between the accelerometer and charge amplifier will not reduce the charge sensitivity of the accelerometer. To illustrate this further, consider Figure 2, the open circuit voltage generator simplified equivalent circuit of an accelerometer.

9
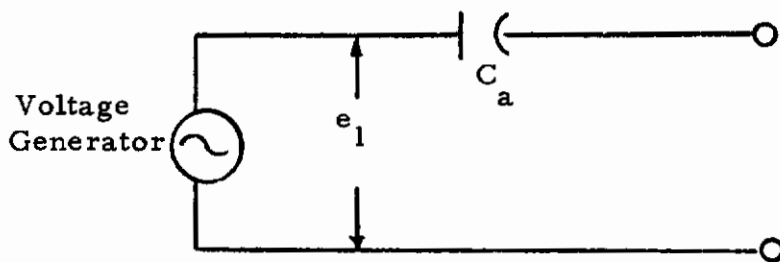
Figure 2. Simplified Voltage Generator Equivalent
Circuit of a Piezoelectric Accelerometer

$$e_1 = \ddot{x} S_2 \qquad\qquad (5)$$

The voltage generated is proportional to the applied acceleration (S_2 is
the sensitivity constant in volts rms per g rms). By connecting the acceler-
ometer to an operational amplifier with a capacitor in the feedback loop, it
is possible to obtain a voltage out of the operational amplifier that is pro-
portional to the applied acceleration and is independent of the shunt capacity
between the accelerometer and the amplifier, as shown in Figure 3.
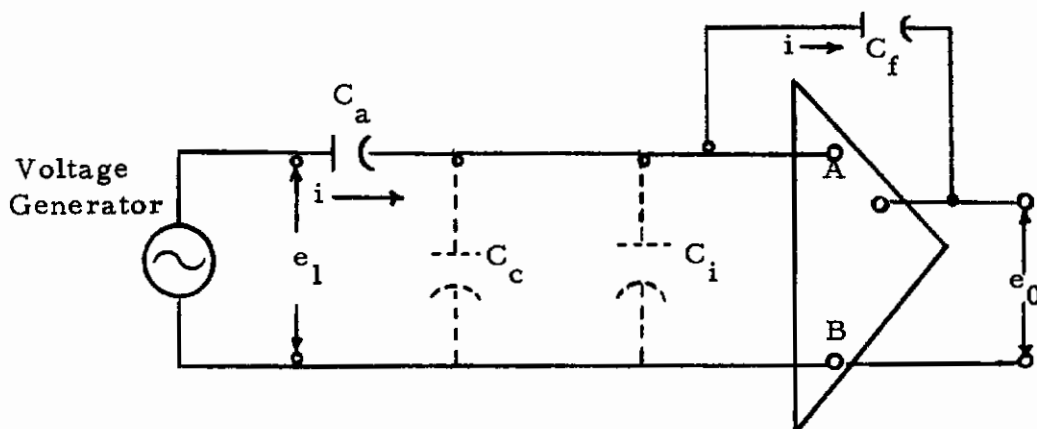
Figure 3. Charge Amplification

10

Since an operational amplifier keeps the current through the feedback impedance (C_f) equal to the current through the input impedance (C_a), there is essentially no current flow or voltage difference between points A and B on the amplifier input. This places point A and the output of the accelerometer essentially at ground potential for practical purposes. Hence, any shunt capacitance occurring between the accelerometer output and the amplifier input is "shorted-out" and does not affect the sensitivity of the accelerometer system.

The output voltage can be shown to be only a function of the accelerometer and feedback capacitances.

$$e_0 = -(i)(Z_f) \tag{6}$$

$$i = \frac{e_1}{Z_a} \tag{7}$$

$$e_0 = -(e_1)\left(\frac{Z_f}{Z_a}\right) = -(e_1)\left(\frac{C_a}{C_f}\right) \tag{8}$$

and, by combining Eqs. (8) and (5),

$$e_0 = -(\ddot{x})(S_2)\left(\frac{C_a}{C_f}\right) \tag{9}$$

The output voltage from the accelerometer system is equal, but of opposite polarity to the product of the applied acceleration and the voltage sensitivity constant of the accelerometer times the ratio of the accelerometer internal capacitance to the feedback capacitance.

In terms of charge sensitivity,

$$S_2 = \frac{e_1}{\ddot{x}} = \frac{q}{\ddot{x}C_a} = \frac{S_1}{C_a} \tag{10}$$

11

and

$$e_0 = -(\ddot{x})(S_1)\left(\frac{1}{C_f}\right) \tag{11}$$

The above discussions on charge amplification have assumed an ideal operational amplifier (infinite input impedance, infinite gain, zero output impedance, zero drift, etc.). Detailed discussion of the errors from using real operational amplifiers is beyond the scope of this report. See Refs. [1, 2, 3]. A number of commercial charge amplifiers have been designed specifically for use with piezoelectric transducers. Versions are available that advertise an allowable source capacitance of up to 100,000 pf for less than $\pm$ 2% gain change while at the same time maintaining a flat frequency response ($\pm$ 5%) between 2 cps and 20,000 cps.

Since the accelerometer signal conditioners of the RTD Sonic Fatigue Facility are voltage amplifiers, all further discussions, except the following brief one, will be limited to this category. It is interesting to note that the accelerometer signal conditioners of the Sonic Fatigue Facility are composed of a high input impedance cathode follower followed by two high quality operational amplifiers that are used for voltage amplification. It may be found beneficial some time in the future to bypass the cathode follower and modify the first operational amplifier to a charge amplifier configuration.

2.3 DRIVEN SHIELD TECHNIQUES

Another method that is frequently used to overcome the attenuation effects of long cables on piezoelectric accelerometer systems is the driven shield technique. In this technique a triaxial cable is used between the accelerometer and the signal conditioner. The inner shield of the triaxial cable is left open at the end near to the accelerometer. By driving this inner shield with a voltage that is in phase with and just slightly lower in amplitude than the voltage appearing between the center conductor and the outer shield, the effective shunt capacitance of the cable can be reduced.

Since cathode followers are frequently used as the input stage of signal conditioners for piezoelectric accelerometers in order to obtain a very high input impedance, the output of the cathode follower provides a convenient source of voltage to drive the inner shield. (Note that the output of the cathode follower will be in phase with its input, and that the gain of the cathode follower will be just slightly less than unity.) Figure 4 is a schematic diagram of a piezoelectric accelerometer system using a driven shield cable.
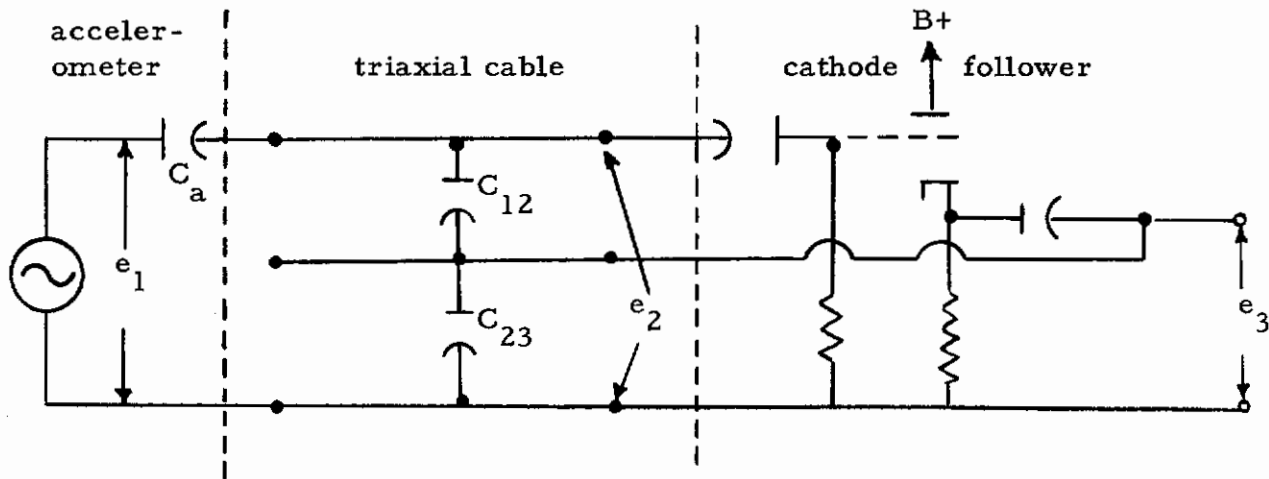
Figure 4. Schematic Diagram of an Accelerometer System Using a Driven Shield Triaxial Cable

13

By making certain simplifying assumptions such as infinite input impedance, infinite grid to cathode impedance, zero output impedance, and mid-frequency band operation for the cathode follower, the equivalent circuit can be re-drawn as shown in Figure 5.
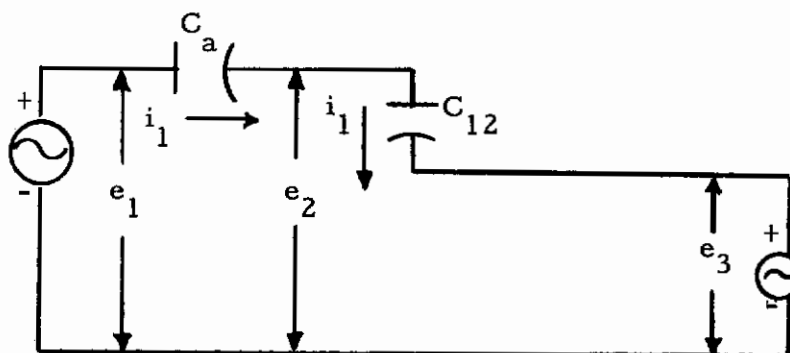
Figure 5. Simplified Equivalent Circuit of an Accelerometer
System Using a Driven Shield Triaxial Cable

To show the effect of the driven shield, the circuit of Figure 5 must be solved for e_2/e_1 .

$$i_1 X_{C_{12}} + e_3 = e_2 \tag{12}$$

$$i_1 = \frac{e_1 - e_2}{X_{C_a}} \tag{13}$$

$$e_3 = A e_2 \tag{14}$$

where

i_1 = the current through C_a and C_{12} in rms amperes

C_{12} = the capacitance between the inner conductor and the inner
shield of the triaxial cable in farads

C_{23} = the capacitance between the inner shield and the outer
shield of the triaxial cable in farads

14

e_2 = the rms voltage at the input to the cathode follower

e_3 = the rms voltage at the output of the cathode follower

A = the gain of the cathode follower (dimensionless)

By combining the above equations, it is found that

$$\frac{e_2}{e_1} = \frac{1}{1 + \frac{C_{12}(1 - A)}{C_a}} \qquad (15)$$

Thus it can be seen that the effective value of shunt capacitance is reduced by a factor of $(1 - A)$ through the use of the driven shield. Obviously, the closer that A approaches unity, the less attenuation there will be due to the cable. The primary problem associated with the use of driven shield techniques is a reduction in the "flat" frequency range of the accelerometer system. This results primarily because the output impedance of the cathode follower is not zero. This decrease in frequency range should not really be a major problem at the Sonic Fatigue Facility. However, the cost of re-wiring the facility to replace the present coaxial transducer to signal conditioner cables with triaxial cables may be prohibitive.

2.4 INTRINSIC INACCURACIES

The intrinsic inaccuracies of accelerometer systems can be defined as the errors occurring when the measurement of acceleration is made under ideal conditions - no environmentally related errors, no usage errors, and no calibration errors. This category of errors can further be broken down into errors due to:

15

(1) Deviations from the theoretical frequency response function due to the amplitude of the applied acceleration;

(2) Deviations from the theoretical frequency response function due to the frequency of the applied acceleration; and

(3) Transverse sensitivity.

Figure 6 shows the basic blocks of an accelerometer system.
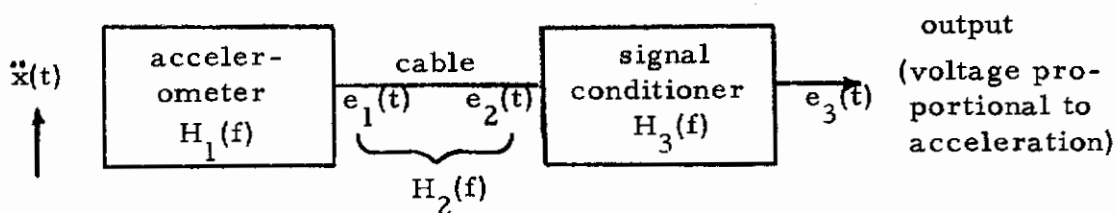
Figure 6. Basic Block Diagram of an Accelerometer System

Ideally, the frequency response functions (see Ref. $\left[12\right]$) $H_1(f)$, $H_2(f)$, and $H_3(f)$ would be constants as given by

$$H_1(f) = K_1 \tag{16}$$

$$H_2(f) = K_2 = 1 \tag{17}$$

$$H_3(f) = K_3 + \frac{e_D}{e_2(t)} \tag{18}$$

where

$H_1(f)$ = the frequency response function between $e_1(t)$ and $\ddot{x}(t)$ in volts/g

$H_2(f)$ = the frequency response function between $e_2(t)$ and $e_1(t)$ (dimensionless)

$H_3(f)$ = the frequency response function between $e_3(t)$ and $e_2(t)$ (dimensionless)

16

$\ddot{x}(t)$ = the instantaneous value of the applied acceleration in g's

$e_1(t)$ = the instantaneous value of the accelerometer output voltage

$e_2(t)$ = the instantaneous value of the voltage at the output of the accelerometer to signal conditioner cable

$e_3(t)$ = the instantaneous value of the signal conditioner output voltage

e_D = the DC drift or bias voltage on the output of the signal conditioner

K_1 = a constant (volts rms per g rms)

K_2 = a constant (dimensionless)

K_3 = a constant (dimensionless gain)

2.4.1 Accelerometer Errors

The factor K_1 is the accelerometer sensitivity factor in volts rms per g rms. There is very little deviation in this factor as a function of the applied acceleration amplitude because the amplitude linearity characteristics of piezoelectric accelerometers are very good. Qualifying "very good" is a bit difficult. Typical amplitude response errors for accelerations up to 100 g's are quoted as "no measurable error" in Ref. [5]. This reference also shows a typical amplitude response error of 2% of full scale for measurements up to the particular full scale acceleration ratings of the accelerometers (300 to 10,000 g's). In Ref. [6], this type of error is called "virtually nonexistent" and a linearity of better than 2% of reading up to 4000 g's is quoted as possible. Furthermore, no intrinsic errors are attributable (Ref. [5]) to resolution, zero shift, and short term sensitivity shift. For further calculations, an error of 2% of reading will be assumed as the error due to all accelerometer amplitude nonlinearities. This assumption will be restricted to acceleration amplitudes between 1 and 100 g's zero to peak.

17

$H_1(f)$ departs rather substantially from a pure constant (K_1) as the frequency of the applied acceleration is varied. In fact, $H_1(f)$ can be quite accurately approximated by the frequency response function of a lightly damped base excited simple mechanical system. See Refs. [7, 8, 9]. The specific frequency response function is the ratio of the relative displacement of the mass to the base acceleration

$$H_1(f) = (C_1) \left[\frac{1}{(2\pi f_n)^2}\right] \left[\frac{1}{\sqrt{\left[1 - \left(\frac{f}{f_n}\right)^2\right]^2 + \left[2\zeta\frac{f}{f_n}\right]^2}}\right] \left[e^{j\phi(f)}\right] \quad (19)$$

$$C_1 = (2\pi f_n)^2 K_1 \quad (20)$$

$$\phi(f) = \tan^{-1}\left[\frac{2\zeta\frac{f}{f_n}}{1 - \left(\frac{f}{f_n}\right)^2}\right] \quad (21)$$

f = the frequency in cps of the applied acceleration

f_n = the undamped natural frequency in cps of the seismic system of the accelerometer

ζ = the damping ratio

C_1 is essentially the sensitivity of the transducer material. It can be seen from Eq. (20) that the over-all accelerometer sensitivity (K_1) decreases as the undamped natural frequency of the accelerometer increases.

The usual rule of thumb in accelerometer usage is that vibration of frequencies up to one-fifth of the mounted natural frequency of the accelerometer can be accurately measured.

18

$$\frac{|H_1(f)|}{K_1} = \frac{1}{\sqrt{\left[1 - (.2)^2\right]^2 + \left[2(.1)(.2)\right]^2}} = 1.04 \quad ; \quad \text{at } \frac{f}{f_n} = .2, \ \zeta \leq 0.1$$

While this is a good rule in general, it should not always restrict the use of accelerometers to frequencies below one-fifth of the mounted resonant frequency of the accelerometer. Certainly, the data reduction process is simplified if frequency response corrections can be ignored, but conceptually, if not yet practically, accelerometers with $\zeta << 1$ can be used to about three times this natural frequency $\left(|H_1(f)|/K_1 \geq 0.1 \text{ for } f \leq 3 f_n\right)$. The problem is not one of intrinsic inaccuracy, but one of calibration inaccuracy (determining the frequency response function accurately), and data reduction inaccuracy (using the frequency response function once if it is known). Figure 7 plots $|H_1(f)|/K_1$ for several values of ζ. Typical values of ζ for piezoelectric accelerometers are .01 to .03. See Ref. [10].

It is usually assumed that there is zero phase shift between the applied acceleration and the output of a piezoelectric accelerometer. This is also a good assumption for frequencies below one-fifth of the mounted resonant frequency of the accelerometer ($\phi < 0.1^\circ$; at $f/f_n = .2$ and $\zeta = .03$). Figure 8 plots $\phi(f)$ for several values of ζ. Nonlinear phase shift ($\phi(f) \neq$ constant) in an accelerometer results in a distorted measurement when the input signal is complex. The only value of ζ for which $\phi(f)$ is linear is $\zeta = 0$. Even this is only piecewise linear with $\phi = 0^\circ$ from $f/f_n = 0$ to 1 and $\phi = 180^\circ$ for $f/f_n > 1$.

From Eq. (21),

$$\phi(f) = \tan^{-1}\left[\frac{2\zeta \frac{f}{f_n}}{1 - \left(\frac{f}{f_n}\right)^2}\right]$$

19
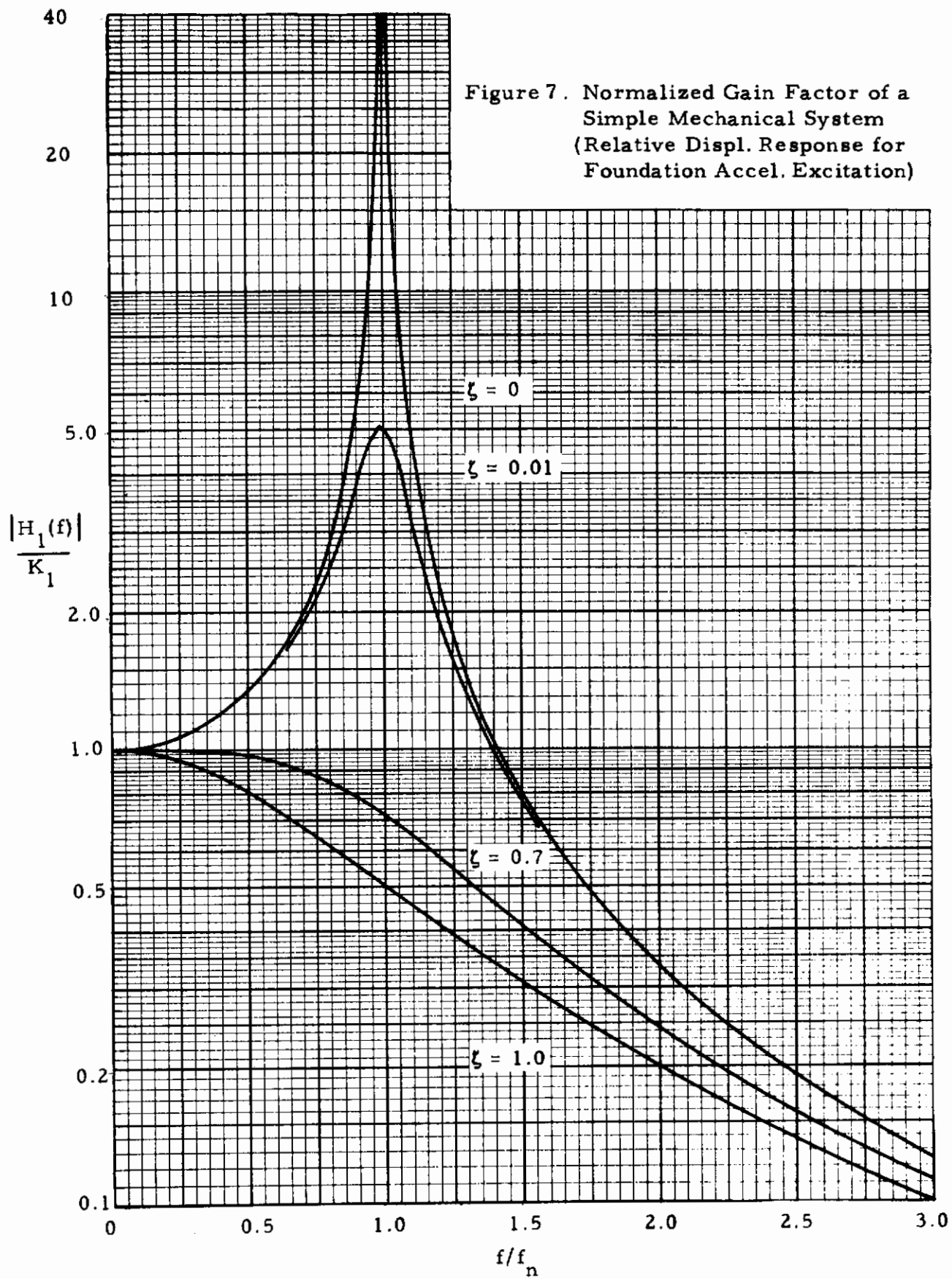
Figure 7. Normalized Gain Factor of a Simple Mechanical System (Relative Displ. Response for Foundation Accel. Excitation)

20
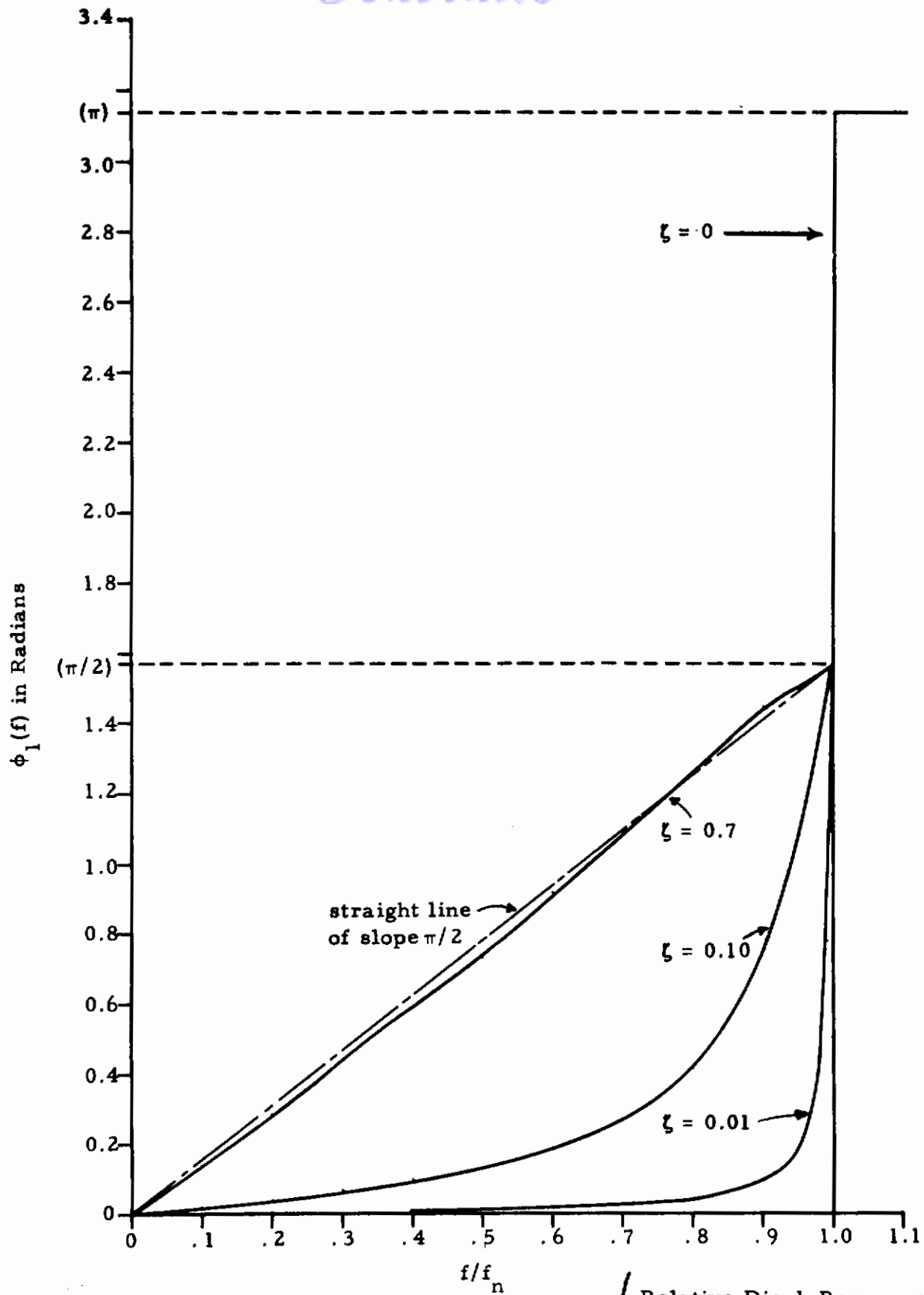
Figure 8. Phase Factor of a Simple Mechanical System $\left(\dfrac{\text{Relative Displ. Response}}{\text{Foundation Accel. Excitation}}\right)$

21

Let $u = \dfrac{f}{f_n}$:

$$\phi(f) = \tan^{-1}\left[\frac{2\zeta u}{1 - u^2}\right]$$

$$\frac{d\phi(f)}{du} = \frac{2\zeta(1 + u^2)}{u^4 + (4\zeta^2 - 2)u^2 + 1} \qquad\qquad (22)$$

If $\phi(f)$ is linear, $d\phi(f)/du$ will be a constant.

$$\frac{2\zeta(1 + u^2)}{u^4 + (4\zeta^2 - 2)u^2 + 1} = \text{constant}$$

The only value of ζ for which this is true is $\zeta = 0$. From Figure 8 it can be seen that $\zeta = .7$ yields a phase shift function that approximates (up to $f/f_n = 1$) the linear phase shift function $(\pi/2f_n)f$. Transducers are frequently designed with $\zeta \approx 0.7$ and a linear phase shift is assumed. However, it must be remembered that the output of a transducer with $\zeta \approx 0.7$ will be delayed in time by $1/4f_n$ seconds from the applied acceleration.

$$\tau = \frac{\phi(f)}{2\pi f} = \frac{\pi f}{\dfrac{2 f_n}{2\pi f}} = \frac{1}{4 f_n}$$

Accurate knowledge of the phase characteristics of accelerometers is of prime importance for cross-correlation and cross-power spectral density analyses.

Transverse sensitivity is another intrinsic inaccuracy of piezoelectric accelerometers. This inaccuracy can be defined as the output of an

22

accelerometer due to an acceleration applied perpendicular to the sensitive axis of the accelerometer. Unlike the preceding two intrinsic accuracy categories, the transverse sensitivity inaccuracy is reasonably well-defined. The magnitude of this inaccuracy is a function of the direction of acceleration application in the plane normal to the sensitive axis. Maximum transverse sensitivities in commercial accelerometers vary from $\pm 1\%$ to $\pm 10\%$. Generally speaking, microminiature accelerometers are more sensitive to transverse acceleration than standard size accelerometers because of the difficulties in holding the same percentage manufacturing tolerances.

2.4.2 Cabling Errors

In the cable connecting the output of the accelerometer to the input of the signal conditioner, the intrinsic inaccuracies due to the applied signal amplitude can be ignored. The only intrinsic inaccuracy that needs to be considered is the variation in K_2 (Eq. 17) with frequency. (Crosstalk between cables will be treated as a usage inaccuracy.)

The cable can be represented by a series of equivalent π section circuits as shown in Figure 9.
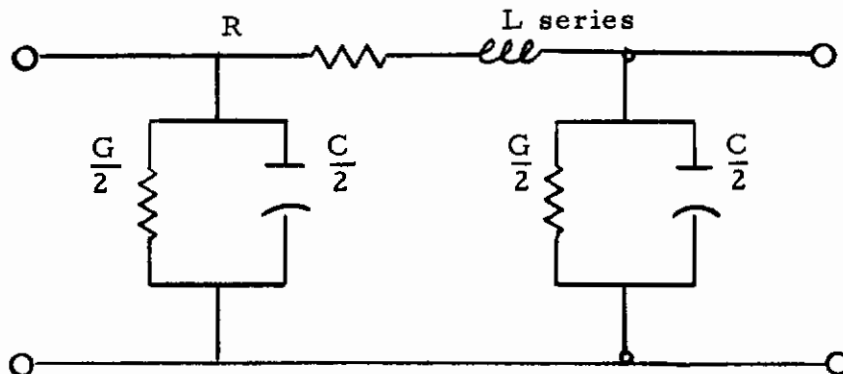
Figure 9. Equivalent π Section

R = series resistance in ohms/ft
G = shunt conductance in mhos/ft
L = series inductance in henries/ft
C = shunt capacitance in farads/ft

23

For the cable length, frequency range, and terminating impedance in use at the Sonic Fatigue Facility, the equivalent circuit of the cable reduces to that of a simple capacitor as shown in Figure 10.

$$C_c = C \times l$$

l is the total cable length
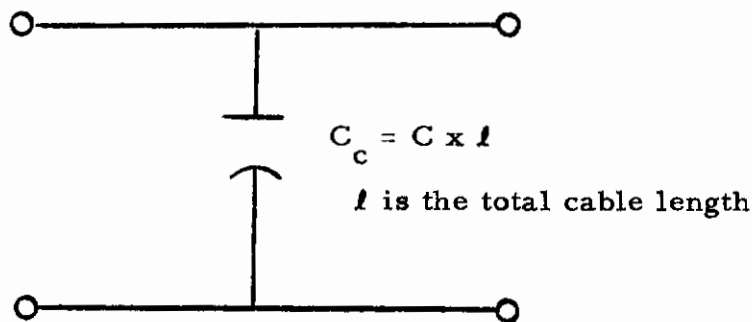
Figure 10. Simplified Equivalent Circuit of an
Accelerometer to Signal Conditioner Cable

Hence, $H_2(f) = K_2 = 1$. However, the value of C_c is quite important when used in the accelerometer/voltage amplifier system because the accelerometer has internal impedance. This effect is shown in Eq. (4).

2.4.3 Signal Conditioner Errors

The signal conditioning equipment in the accelerometer channels is composed of an impedance converter (cathode follower), an attenuator, two operational amplifiers, and a differential isolator. (The automatic gain switching features of the signal conditioners at the RTD Sonic Fatigue Facility will be discussed in a later report.) Figure 11 is a block diagram of the signal conditioner.

24
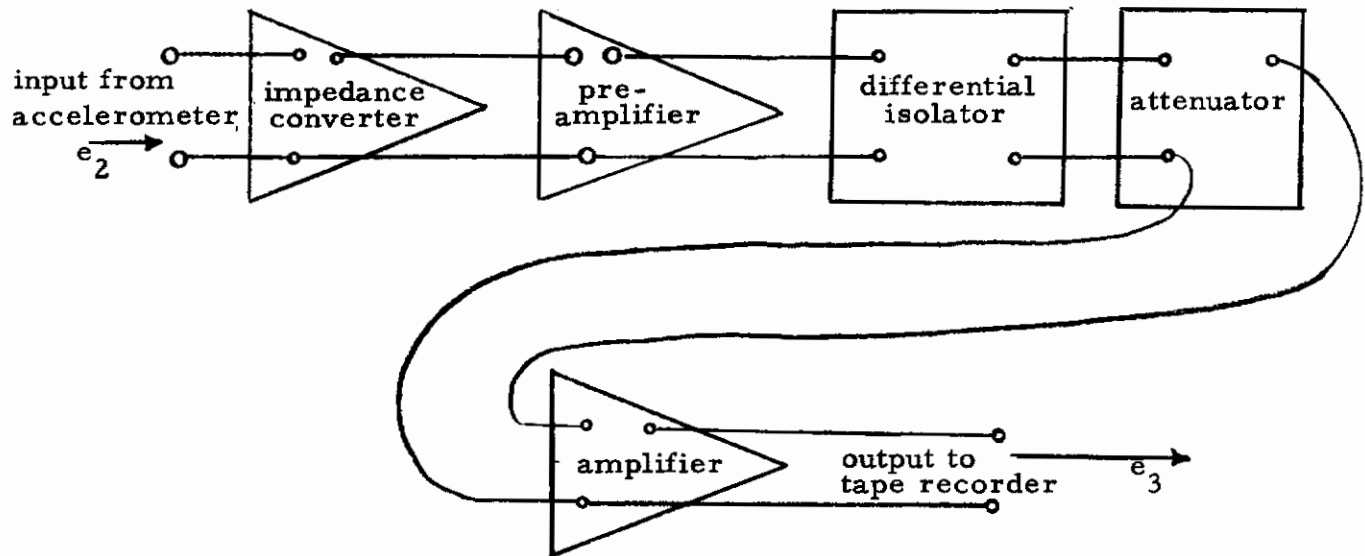
Figure 11. Block Diagram of an Accelerometer Signal Conditioner

From Eq. (18), the ideal frequency response function for the signal conditioner is

$$H_3(f) = K_3 + \frac{e_D}{e_2}$$

The intrinsic inaccuracies of the signal conditioner can also be separated into three categories - those due to the amplitude of the applied input signal, those due to the frequency of the applied input signal, and those due to the variation of K_3 and/or e_D with time. Since the signal conditioner is composed of a number of blocks, the combined effects of the individual inaccuracies of each block must be determined. Unfortunately, there is not sufficient information available in the operating manuals for the individual circuit "blocks"; so it will be necessary to experimentally determine these inaccuracies.

25

Amplitude nonlinearity and dynamic range (signal to noise ratio) are the two factors that cause amplitude related intrinsic inaccuracies in signal conditioners. (There are no pure resolution problems.) The total signal conditioner amplitude nonlinearity must be measured. Even if the percent contribution of each block is known, calculations cannot be made unless the type of nonlinearity is known. The amplitude nonlinearity inaccuracy of the signal conditioner will probably be low. One might anticipate the inaccuracy to be at its maximum with accelerometers of high sensitivity subjected to high acceleration levels, since this will require the impedance converter and particularly the first amplifier to work at high voltage levels. In fact, it will probably be difficult to maintain a sensitivity of 10 mv/g at the input to the attenuator with accelerometers of moderately high sensitivity. See Ref. [11].

Example: Assume that the acceleration sensitivity at the input to the impedance converter is 15 mv/g. The maximum output voltage of the first amplifier is 50 volts zero to peak. The gain of the impedance converter is .99 and the gain of the first amplifier is 100; so the total gain is $(.99)(100) \approx 100$. Therefore, the maximum allowable input voltage to the impedance converter is 50V/100 = 0.5 volts zero to peak. The maximum allowable acceleration level is then

$$\frac{0.500V}{0.015V/G} = 33.3 \text{ g's zero to peak, a value which is very likely to be}$$

exceeded during high level sonic testing.

The dynamic range of the signal conditioner, over the useful frequency range, can never improve over its value at the output of the impedance converter since both the signal and the noise will be equally amplified between this point and the signal conditioner output. The value of the noise voltage on the output of the signal conditioner (see Ref. [11]) is:

26

$$e_N = (100) \sqrt{\left[(100)(A)(z)\right]^2 + y^2} \qquad (23)$$

where

$$z = \sqrt{e_a^2 + e_b^2 + \left(\frac{e_c}{100}\right)^2} \qquad (24)$$

e_N = output noise voltage of the signal conditioner in volts rms

y = equivalent input noise voltage of the second amplifier in volts rms

A = total "gain" in the normalizing and automatic attenuators

e_a = output noise voltage of the impedance converter in volts rms

e_b = equivalent input noise voltage of the first amplifier in volts rms

e_c = equivalent input noise voltage of the differential isolator in volts rms

Since the signal conditioner output is restricted to a maximum of ± 1 volt, the total dynamic range (maximum allowable instantaneous voltage divided by the rms noise voltage), see Ref. [12], can be written as follows.

$$(S/N)_{total} = \frac{1}{(100)\sqrt{\left[(100)(A)(z)\right]^2 + y^2}}$$

Clearly, the smallest dynamic range will occur when A is at its maximum value ($A = 1$). Under this condition the voltage into the signal conditioner for full scale output will be only 0.1 mv zero to peak.

Determining the usable dynamic range requires a priori knowledge of the probability density function of the signal and a specified tolerance on the allowable error in the signal conditioner. (This is thoroughly discussed in Ref. [12].) Measurement of the output noise voltage should be made with a dummy accelerometer (capacitance $\approx C_a$) connected to the impedance converter input.

Measurement of the actual gain and phase shift variations of the signal conditioner with the frequency of the input signal is straightforward and will not be discussed here, except to point out that the phase information cannot be neglected if cross-correlation or cross-power spectral density analyses are to be performed.

Any variation in gain of the signal conditioner during data taking will be reflected in a directly related measurement inaccuracy (p% variation in K_3 results in p% error in the data). Obviously, gain stability is quite important and every block in the signal conditioner shows equally in over-all gain stability. A variation of 1% in the attenuation of an attenuator is just as important as the 1% variation in the gain of an amplifier.

Variation in e_D , theDC bias voltage on the signal conditioner output, with time can cause several kinds of inaccuracies. For acceleration measurements, e_D will nominally be zero. Departure of e_D from zero can cause inaccuracies by introducing a nonzero mean value and by decreasing the ideal dynamic range in one direction (clipping of output signals of one polarity at less than 1 volt zero to peak). The total drift voltage at the output of the signal conditioner is (see Ref. $\left[11 \right]$):

$$e_D = (100) \left\{ \left[(e_{aD} + e_{bD})(100) + e_{cD} \right] (A) + y_D \right\} \qquad (25)$$

where

e_D = output of the signal conditioner, due to drift, in volts DC

e_{aD} = output of the impedance converter, due to drift (leakage through the shunt resistance of the output coupling capacitor) in volts DC

e_{bD} = equivalent input to the first amplifier, due to drift, in volts DC

e_{cD} = equivalent input to the differential isolator, due to drift, in volts DC

y_D = equivalent input to the second amplifier, due to drift, in volts DC

28

The most serious drift problem is likely to occur from e_{aD} not being negligible.

2.4.4 Other Errors

In addition to the individual intrinsic inaccuracies, one must consider the accelerometer, cable, and signal conditioner as a system. When treated as a system, the shunt capacitance of both the interconnecting cables and the signal conditioner input alter the over-all accelerometer system frequency response function in two manners. First, as shown in Eq. (4), the over-all system sensitivity is reduced by these capacitances. Secondly, the low frequency response of the system is flattened. See Figure 12.
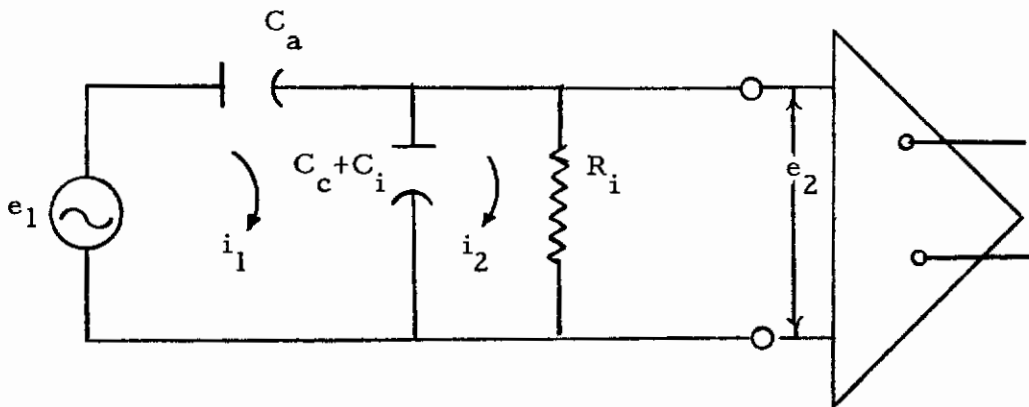
Figure 12. Simplified Voltage Generator Equivalent Circuit of an Accelerometer Cable and Voltage Amplifier

R_i = the input resistance of the signal conditioner in ohms

f = the frequency of the applied acceleration in cps

$$\frac{e_2}{e_1} = \left(\frac{C_a}{C_a + C_c + C_i} \right) \left[\frac{1}{1 + \frac{1}{2\pi jf(R_i)(C_a + C_c + C_i)}} \right] \tag{26}$$

29

From inspection of the above equation, the sensitivity attenuation factor is seen to be $\left(\dfrac{C_a}{C_a + C_c + C_i} \right)$. Also, the larger the $R(C_a + C_c + C_i)$ product, the less attenuation there will be at low frequencies.

2.5 ENVIRONMENTAL INACCURACIES

As stated in the introduction, the inaccuracies due to exposure to environments will be limited to those environments and environmental ranges that can reasonably be expected to be present in the Sonic Fatigue Facility. Since the transducer system is used within an environmentally controlled building, the climatic environments will be limited in range. However, the elements of the transducer system inside of the test chamber will be subjected to extreme dynamic environments. Specifically, the climatic environments that can cause inaccuracies are temperature and relative humidity. The dynamic environments that can cause inaccuracies are vibration and high intensity acoustics.

The accelerometers and cable inside the test chamber will be subjected to the most severe temperature fluctuations. The extremes will be assumed to be at 50°F. and 100°F. The signal conditioners are located in a well airconditioned room; therefore, this temperature will be assumed to be limited between 60°F. and 80°F.

In Figure 13, the total accelerometer system is shown.
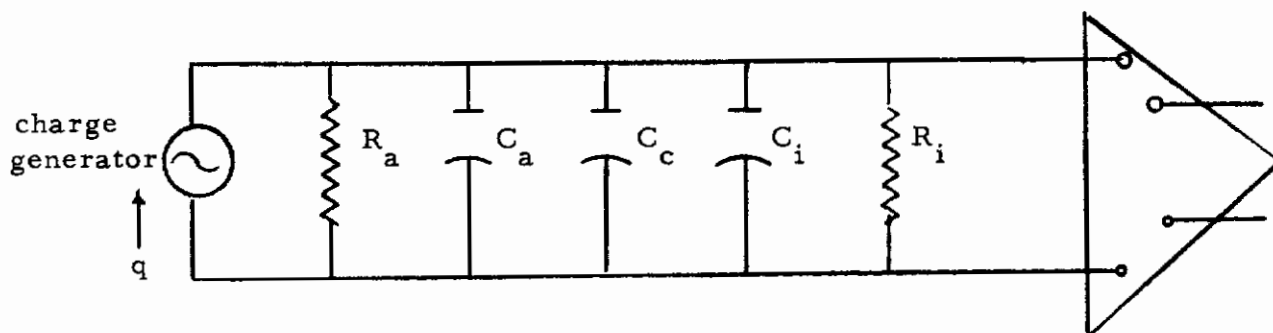
Figure 13. Equivalent Circuit of a Piezoelectric Accelerometer System

30

Note that R_a, the shunt resistance of the accelerometer is included. This resistance is so high at room conditions that it was neglected in the previous intrinsic accuracy discussion.

All three of the accelerometer parameters (S_1, C_a, and R_a) vary with temperatures. See Refs. [13, 14] . The actual resultant accelerometer voltage sensitivity (S_2) and shunt resistance variations with temperature are strongly dependent on the particular piezoelectric material used and the accelerometer construction. Typical variations of S_2 with temperature range from .01%/$^\circ$F. to 1.0%/$^\circ$F. See Ref. [5]. For a 50°F. temperature variation, this results in anywhere from a 0.5% error to a 50% error in accelerometer sensitivity. The variation in both internal shunt resistance and internal capacitance of the accelerometer will result in a change in the low frequency response of the accelerometer system. For a given low frequency, the value of attenuation at room temperature will be decreased as the temperature decreases and increased as the temperature increases. From the above it can be seen that the temperature sensitivity of an accelerometer can be a very important factor even for laboratory measurements.

The effects of temperature on the accelerometer to signal conditioner cable can be neglected in the above temperature ranges. This fact helps to minimize the variation in acceleration sensitivity at the input to the signal conditioner (see Ref. [13]).

Temperature variations at the signal conditioner can result in variations in the input impedance, gain, frequency response, DC drift voltage on the output, and the noise level. The magnitudes of this variation will have to be determined experimentally. The fact that the signal conditioner racks are cooled by forced air will help to minimize the temperature variation of the signal conditioner once they have stabilized. Minimizing the allowable fluctuation in this forced air temperature and in the room air

31

temperature, as well as maintaining an adequate flow rate of forced air, will reduce the errors due to temperature. Also, since the active elements in the signal conditioners have large amounts of negative feedback, the gain variations should be small.

Relative humidity, up to 100% but not including rain, should not cause any inaccuracies in the use of piezoelectric accelerometer systems. Piezoelectric materials are sensitive to humidity, but almost all commercial accelerometers have epoxy or metal to metal seals. The cable and the signal conditioner should both be insensitive to humidity. The only problem that should occur is if the connectors of the cable are not properly sealed so that moisture can condense on their surface and effectively shunt the signal conditioner input resistance. This will result in an attenuation of the low frequency response.

The greatest environmental inaccuracy may well result from the acoustic sensitivity of the piezoelectric accelerometer systems. The range of spurious acceleration output that can be expected for 180 db of broadband (2 cps to 10 kc) acoustic excitation varies from 22 to 50 g's rms. These values are extrapolations of the acoustic sensitivities quoted in Refs. [15, 16, 17, 18].

To the author's knowledge, there has not been an extensive experimental study of the response of accelerometers to high intensity acoustic excitation since 1958 (see Ref. [19]). Such a program may be well worth considering for performance in the RTD Sonic Fatigue Facility. First, this would give an empirical measure of the amount of spurious response for the particular transducers to be used at this facility. Second, it would permit selection of the optimum accelerometers for use in the Sonic Fatigue Facility; and third, it would permit checking of present theories on the proportionality of the spurious acceleration response to the sound pressure level. Since the frequency response function of a piezoelectric accelerometer is that of a lightly damped simple mechanical system (see Eq. 19),

32

its spurious response to broadband acoustic noise can be somewhat minimized by increasing its natural frequency, and/or increasing its damping, preferably the former. Increasing the natural frequency will move the peak in the frequency response of the accelerometer above the acoustic frequencies and increasing the damping will decrease the magnitude of the peak.

The cable, if properly used, will be insensitive to acoustic excitation. Since the active elements of the signal conditioners are primarily vacuum tubes, the signal conditioners will be sensitive to acoustic excitation and vibration transmitted through the building. Whether this will be a problem or not depends on the effectiveness of the acoustic and vibration isolation between the test chamber and the signal conditioners.

2.6 USAGE INACCURACIES

Usage inaccuracies are one of the most profitable areas of inaccuracy causes to be studied because steps can be taken to minimize these inaccuracies, although they cannot be eliminated.

2.6.1 Accelerometer

As with any transducer, piezoelectric accelerometers should exactly follow the motion being transduced without altering the motion. Since the accelerometer has finite mass, this is not possible. A rule of thumb has been to restrict the transducer mass to one-tenth or less that of the object being measured. This criteria results in a rigid body acceleration measurement error of at most 10%. With the advent of microminiature accelerometers, weighing only fractions of a gram, the errors due to finite mass have been considerably reduced. However, one should attempt to estimate the effect of the accelerometer mass on the measurement.

33

Selecting the proper location for the accelerometer is another usage problem. Only very general guidelines can be given because each particular test will have unique requirements as to where measurements should be made, and will also probably have unique problems in placing an accelerometer on that location. In general, if no other requirements are specified, the accelerometers should be located on rigid structures, near attachment points, where there is no problem with the accelerometer colliding with adjacent structures.

Mounting the accelerometers, once a point for measurement has been selected, is another usage problem. The attachment can either be directly to the point, or indirectly through some type of mounting block or fixture. Direct attachment is preferable since it removes another source of possible inaccuracy. Methods of attachment that are frequently used include bolts, studs, glue, dental cement, and double backed tape. When using bolts or studs (other than those that are integral with the accelerometer or have shoulders), one must be careful not to bottom the bolt or stud in the mounting hole of the accelerometer as this will distort the piezoelectric crystal and cause an inaccurate output or even damage to the accelerometer. When mounting accelerometers with any screw type of device, the accelerometer should always be torqued to the value recommended by the manufacturer in order to assume a firm attachment without damaging the accelerometer, and to remove the effects of torque sensitivity. Glue, such as Eastman 910, dental cement, and double backed tape are extremely convenient methods for attaching accelerometers. One investigation (Ref. [20]) showed that there was little variation in sensitivity from the normal mounting for frequencies up to 2 kc. This same reference showed that Permacel 50 double backed tape transmitted acceleration linearly up to 400 g's zero to peak, and that Eastman 910 cement can be used linearly up to 1000 g's zero to peak. These cements or tapes will generally not

34

withstand high shear loads, so one must be careful not to use this type of attachment where high transverse accelerations are likely.

Frequently it is not possible to attach the accelerometer directly to the desired measurement point because of physical problems such as surface roughness or shape. In these cases a mount or fixture is necessary. The frequency response function of these mounts and their transverse sensitivity should always be determined before they are used. These mounts can be a large source of error.

Regardless of the type of attachment used, the surface that mates with the accelerometer should be smooth and the accelerometer mounting surface should be truly perpendicular to the axis in which vibration measurements are desired. As shown in Figure 14, if the accelerometer is misaligned from the defined axis A-A by an angle θ, the output will be B-B and the resulting percent error will be:

$$\% \text{ error} = (100)(1 - \cos \theta) \qquad (27)$$
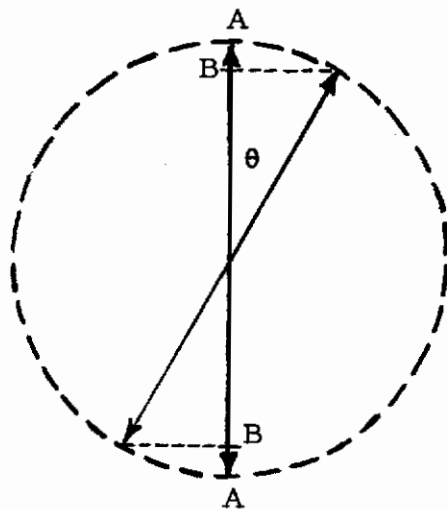
Figure 14. Misalignment in Accelerometer Mounting

2.6.2 Cable

Care in selection of and use of the cable between the accelerometer and signal conditioner can also reduce usage errors appreciably. The most common problem occurring in use of these cables is contamination of the connectors (accelerometer and signal conditioner connectors in addition to the cable connectors). Since a high input impedance is required on the output of the accelerometer, as previously shown, contamination of the connectors will result in a greatly reduced shunt resistance across the cables and degradation of the low frequency response of the accelerometer system. Dirt, moisture, and oils from handling of the accelerometer or cable are a very frequent source of this contamination. All connectors should be carefully cleaned per the manufacturers' instructions just prior to usage.

Internal noise generated by motion of the cable is another possible source of usage inaccuracy. Separation of the dielectric from either the center conductor or shield will result in triboelectric cable noise (see Ref. [21]). Since the cable is attached to the accelerometer, this cable noise will be of the same frequency as the acceleration and will be indistinguishable from the accelerometer output. In fact, with accelerometers of low sensitivity, the cable noise can predominate. Care should be taken to select cables that are relatively insensitive to this effect. (See Ref. [22] for the results of a test of several representative types of low noise cables.) Clamping the cable to restrict motion is an effective way to reduce cable noise. Care must be taken though not to restrict the motion of the accelerometer by clamping the cable too closely to it.

Since the instrumentation system at the RTD Sonic Fatigue Facility has a large number of transducer cables routed through the same conduit, the signal crosstalk between cables should be measured (see Ref. [23] for one measurement method). This should be accomplished prior to usage for testing so that steps can be taken to reduce the crosstalk if it is too high.

36

2.6.3 Signal Conditioner

Another common usage inaccuracy occurs from ground loops. This situation can occur whenever the accelerometer system is grounded at more than one point. If there are differences in the voltage potential between the ground points, these voltage differences will be superimposed on the signal voltage. The most effective method of eliminating problems from ground loops is to isolate the entire system from ground and then ground the output of the signal conditioner at the tape recorder input. This method is called "floating." A number of other techniques are available to minimize ground loop problems. Among these techniques are differential amplification, guard shields, input isolation, output isolation, and various combinations of the preceding. The primary technique used at the Sonic Fatigue Facility is output isolation. The output of the preamplifier stage is connected to the differential isolator whose output is connected in turn to the second amplifier. The purpose of the differential isolator is to couple the output of the preamp to the second amplifier with "no" capacitive coupling between the two amplifiers. (It is essentially a transformer with frequency response down to DC). Thus, if the ground loop voltage is developed equally across the high and ground sides of the input, none of this voltage will be transformed into the output stage. If the transducers and the cable connectors are isolated from ground, floating operation of the input can also be achieved at the RTD Sonic Fatigue Facility. This should help further reduce the ground loop or common mode voltage on the output of the signal conditioner.

2.6.4 Calibration Inaccuracies

A "poor quality" accelerometer system can yield accurate measurements, and conversely, a "high quality" accelerometer system can yield inaccurate measurements. Both of these statements depend on the accuracy and thoroughness of the calibrations performed. Clearly, the most accurate

measurements can be made with a high quality accelerometer system that is both accurately and thoroughly calibrated. However, for many tests it will be a waste of time to thoroughly calibrate all of the accelerometer systems. In fact, a one point (one amplitude value at one frequency) calibration may be satisfactory for many tests. The minimum number of calibration points (frequencies and amplitudes) versus percent error cannot be plotted until certain of the inaccuracies are empirically measured.

There are numerous methods by which calibration can be performed. Most of these involve variations of manners in which the excitation is provided. These can be reduced to two basic methods. The first is the system calibration method. The accelerometer is subjected to a known acceleration excitation and the voltage output of the signal conditioner is measured. In the second method, the voltage sensitivity of the accelerometer and its source impedance are measured; the frequency response function and input impedance of the signal conditioner are measured; and the total system sensitivity is calculated. The system calibration is preferable, if it can be conveniently performed.

Periodically, the accelerometer systems should be thoroughly calibrated with instruments whose calibrations are traceable to the National Bureau of Standards to check the stability of the sensitivity.

Perhaps the best manner to conveniently calibrate accelerometers or accelerometer systems over a wide frequency range is by the "back to back" calibration method. See Figure 15. The accelerometer system to be calibrated is mounted on one side of a very rigid fixture. Directly opposite this accelerometer, and on the other side of the fixture, an accelerometer that has been calibrated by NBS is attached. The fixture is then vibrated by a shaker system and the ratio of the output voltage from the accelerometer system being calibrated to the output voltage of the

38

calibrated accelerometer system is measured. The sensitivity of the accelerometer system being calibrated is then the product of this ratio and the sensitivity of the calibration accelerometer system.
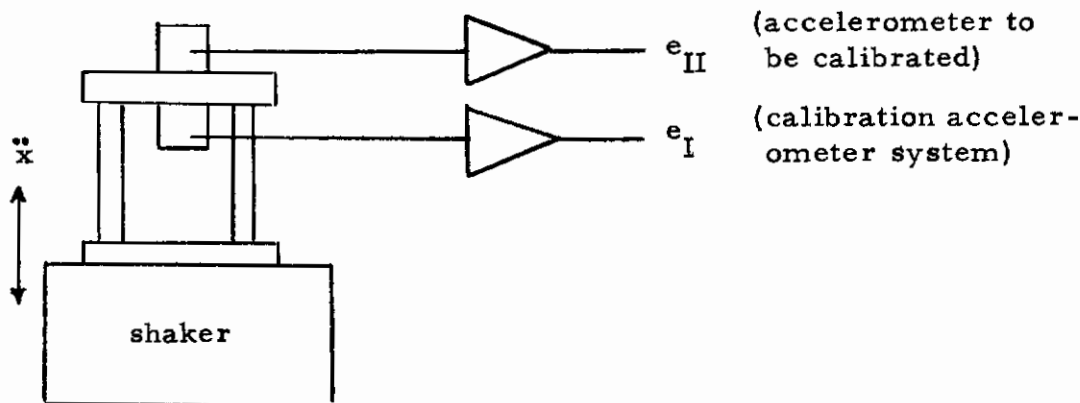
Figure 15. Back to Back Accelerometer Calibration

$$S_{II} = \frac{|e_{II}|}{|e_I|} S_I \quad ; \quad \text{in volts rms/g's rms}$$

The major limitations on this method are:

(1)   An upper frequency limit where the motion of both accelerometers are not identical (fixture resonance).

(2)   The maximum acceleration amplitude is limited by the shaker capabilities (100 g's or less).

(3)   The accuracy with which the sensitivity of the calibration accelerometer is known. (NBS will calibrate piezoelectric accelerometers to an accuracy of 1% up to 900 cps and 2% from 900 to 10,000 cps).

39

3. SOUND MEASURING SYSTEMS

As with accelerometers, there are many types of microphones and signal conditioners used to measure sound pressure levels. Some of the most common types of microphones, along with their major advantages and disadvantages are listed in Table 2. At the present time there is no one type of microphone system that is clearly ideal for high intensity acoustic measurements. Such an ideal microphone system would have a very high frequency cutoff, no phase shift, a wide dynamic range, a high output sensitivity, small size and weight, perfect omnidirectional response, and total insensitivity to other environments. The most common type of microphone used for the measurement of high intensity sound during laboratory testing is the condenser microphone. This type of microphone is popular because of its wide frequency range, wide dynamic range, and sensitivity stability. In recent years, the usage of piezoelectric micro-phones for the measurement of high intensity sound has increased. This type of microphone has several advantages:

(1)   insensitive to humidity

(2)   operates properly in the presence of rapid changes in the ambient pressure

(3)   small size (entire signal conditioner can be remotely located)

Since piezoelectric microphones will be used at the Sonic Fatigue Facility, all further discussions in this section will be limited to this type of microphone.   Also, since the piezoelectric microphones are so similar in construction, operation, and usage to the piezoelectric accelerometer systems discussed in Section 2, detailed discussions in the following sections will be restricted to the points where there are signifi-cant differences between the two classes of transducers. Similarly, since the identical cabling and signal conditioners are used, there will be no discussions of these matters.

40

Table 2. Comparison of Microphones for High Intensity Sound Measurements

	Operating Principle	Major Advantages	Major Disadvantages
1.	Piezoelectric	1. Small size and weight 2. Self-generating 3. Wide dynamic range	1. High output impedance 2. Shunt capacitance of cabling can reduce output voltage 3. Sensitive to vibration
2.	Variable Capacitance (Condenser)	1. Wide dynamic range 2. Constant gain factor over a wide frequency range 3. Highly stable sensitivity	1. Can malfunction in high humidity 2. High output impedance 3. Not self-generating (excitation voltage required) 4. Fragile
3.	Moving Coil (Dynamic)	1. Low output impedance 2. Self-generating 3. High sensitivity	1. Sensitive to temperature 2. Sensitive to electromagnetic fields 3. Relatively low maximum SPL limit
4.	Differential Dynamic (Ribbon)	1. Permits pressure gradient measurement 2. Low output impedance 3. Self-generating	1. Sensitive to temperature 2. Sensitive to electromagnetic field 3. Relatively low maximum SPL limit 4. Fragile

41

3.1 INTRINSIC INACCURACIES

The intrinsic inaccuracies of a microphone system can be found in one of the following categories:

(1) Deviations from the theoretical frequency response function due to the amplitude of the applied sound pressure level.

(2) Deviations from the theoretical frequency response function due to the frequency of the applied sound pressure level.

(3) Deviations from the theoretical frequency response function due to the angle of the incidence of the sound upon the microphone.

Figure 16 is a simplified block diagram of a microphone system.
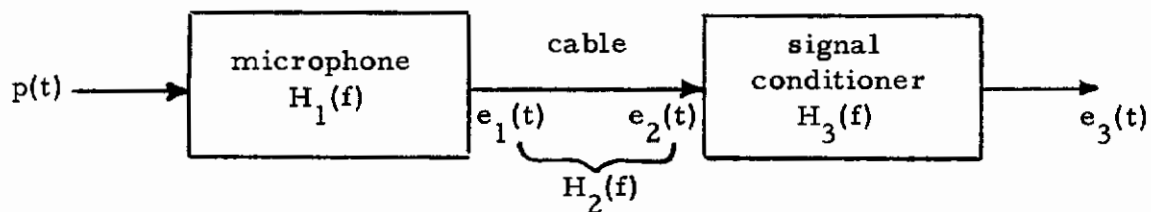
Figure 16. Basic Block Diagram of a Microphone System

The "ideal" frequency response functions would be constants as given below:

$$H_1(f) = K_1$$

$$H_2(f) = K_2 = 1$$

$$H_3(f) = K_3 + \frac{e_D}{e_2(t)}$$

42

where

$H_1(f)$ = the frequency response function between $e_1(t)$ and $p(t)$ in volts per psi

$H_2(f)$ = the frequency response function between $e_2(t)$ and $e_1(t)$ (dimensionless)

$H_3(f)$ = the frequency response function between $e_3(t)$ and $e_2(t)$ (dimensionless)

$p(t)$ = the instantaneous applied sound pressure in pounds per square inch (psi)

$e_1(t)$ = the instantaneous voltage out of the microphone

$e_2(t)$ = the instantaneous voltage out of the cable

$e_3(t)$ = the instantaneous voltage out of the signal conditioner

e_D = the DC bias voltage on the output of the signal conditioner

K_1 = the microphone sensitivity factor in volts rms per psi rms

K_2 = the cable attenuation factor (dimensionless voltage ratio)

K_3 = the signal conditioner gain

The amplitude linearity characteristics of piezoelectric microphones, as with piezoelectric accelerometers, are quite good. Sound pressure levels in the order of 200 db (re .0002 µbar) can be measured with less than 5% deviation in $H_1(f)$ from linearity [24, 25]. To appreciate the magnitude of 200 db, it should be remembered that this corresponds to a pressure of approximately 30 psi or twice that of atmospheric pressure.

The departure of $H_1(f)$ from K_1 as the frequency of the applied sound pressure is varied depends on the particular model of microphone being used. $H_1(f)$ for piezoelectric microphones can be approximated by the frequency response function of a single degree-of-freedom system, but the percent of critical damping varies considerably between different models. The specific single degree-of-freedom frequency response function that approximates $H_1(f)$ is the ratio of the relative displacement response to a force excitation.

43

From Ref. [12],

$$H_1(f) = \frac{K_1 e^{j\phi_1(f)}}{\sqrt{\left[1 - \left(\frac{f}{f_n}\right)^2\right]^2 + \left[2\zeta\frac{f}{f_n}\right]^2}} \qquad (28)$$

$$\phi_1(f) = -\tan^{-1}\left[\frac{2\zeta\frac{f}{f_n}}{1 - \left(\frac{f}{f_n}\right)^2}\right] \qquad (29)$$

where

f = the frequency of the applied force in cps

f_n = the undamped natural frequency of the seismic system of the microphone

ζ = the damping ratio

For those piezoelectric microphones that have very small damping, the discussions previously made on piezoelectric accelerometers apply. (Use of the transducer for frequencies up to one-fifth of its natural frequency is a good rule of thumb. At $f/f_n = .2$, $H_1(f)/K_1 \approx 1.04$, and $\phi(f) < 0.1^o$.) However, for those piezoelectric microphones with appreciable damping, the above rule of thumb does not apply. The allow-able value of f/f_n for a given percent deviation of $|H_1(f)|$ from K_1 is strongly dependent on the damping ratio ζ. Figure 4 of Ref. 8 plots $|H(f_1)|/K_1$. (Note that this curve in Ref. [8] was derived for the ratio of relative displacement to base acceleration, but also applies to the force excited single degree-of-freedom system (compare Eqs. (20) and (28)).

44

When the damping is appreciable, the phase shift in the microphone becomes important. The degree of importance depends on the type of data being measured, and the type of analysis that will be performed on the data. For cross-correlation and cross-power spectral analyses, this could be a significant problem. There will not only be a phase shift between the applied sound pressure and the voltage out of the microphone, but this phase shift may well be nonlinear ($\phi(f) \neq$ constant). In Ref.[8, Figure 5], $\phi(f)$ curves are plotted for various values of damping. (Use ordinate labeled "Const. Disp.".)

One must be careful not to confuse $H_1(f)$ of a real microphone with the "free field response" of the microphone. $H_1(f)$ is the pressure response. (See Ref. [26].) The pressure response is the ratio of the voltage out of the microphone divided by the actual pressure occurring on the sensitive surface of the microphone. The free field response is the ratio of the voltage out of the microphone to the pressure that would have occurred in the spot where the microphone was located - if the microphone had not been there, or if the microphone had been infinitesimally small.

$$\left| H_{FF}(f) \right| = \frac{e_1}{P_a} \tag{30}$$

$$\left| H_1(f) \right| = \frac{e_1}{P_b} \tag{31}$$

where

$H_{FF}(f)$ = the free field response function of a microphone in volts rms per psi rms

$H_1(f)$ = the pressure response of the same microphone in volts rms per psi rms

e_1 = the output of the above microphone in volts rms

P_a = the pressure in a specific location in a given sound field in psi rms

45

P_b = the pressure on the sensitive surface of the above microphone when positioned in the same location and in the same sound field as described for P_a (units of psi rms)

In practice,

$$P_b \geq P_a \tag{32}$$

Therefore,

$$\left| H_{FF}(f) \right| \geq \left| H_1(f) \right| \tag{33}$$

These two frequency response functions will be identical at low frequencies, but can be vastly different at high frequencies. (A high frequency shall be considered to be one where the wave length of the sound is not large compared to the physical dimensions of the microphone.) Reflection of the pressure waves from the sensitive surface of the microphone causes this pressure difference.

These two frequency response functions are related as follows for 0° angle of incidence:

$$H_{FF}(f) = H_1(f) \cdot H_S(f) \tag{34}$$

$$\left| H_{FF}(f) \right| = \left| H_1(f) \right| \cdot \left| H_S(f) \right| \tag{35}$$

$$\phi_{FF}(f) = \phi_1(f) + \phi_S(f) \tag{36}$$

where

$H_{FF}(f)$ = the free field frequency response function of a microphone in volts per psi

$H_S(f)$ = the dimensionless frequency response function relating the free field and the pressure response of a microphone. (This is a function of the size and shape of the microphone.)

$\phi_{FF}(f)$ = the free field phase factor in degrees

$\phi_S(f)$ = the phase factor of $H_S(f)$ in degrees

46

Since the free field frequency response function $H_{FF}(f)$ is usually of more importance for acoustic testing than the pressure response frequency function $H_1(f)$, it will usually be necessary to determine $H_{FF}(f)$ if the microphone is used to measure sound pressure levels at frequencies where $H(f_1) \neq H_{FF}(f)$. Normally $H_1(f)$ is measured and $H_{FF}(f)$ is calculated by use of $H_S(f)$.

Another intrinsic inaccuracy of microphones, directivity, is also related to the dimensions of the microphone. At frequencies where the wave lengths of the sound is not large compared to the dimensions of the microphone, the gain factor of the microphone, $|H_{FF}(f)|$, is sensitive to the orientation of the microphone to the sound. At low frequencies the response of the microphone will be independent of its orientation to the sound. See Figure 17.

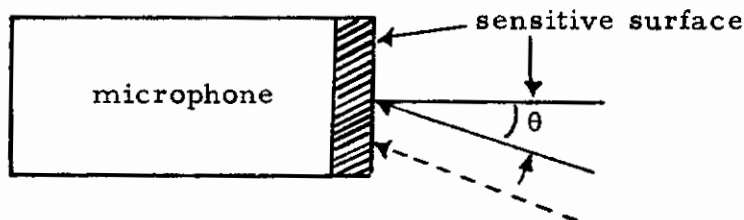Figure 17. Microphone Oriented θ Degrees from Sound Wave

As the wave length of the sound approaches the physical dimensions of the microphone, the free field frequency response function becomes dependent upon the angle of incidence, θ, of the sound wave upon the sensitive surface of the microphone. (See Refs. [26, 30].)

$$H_{FF}(f) = H_1(f) \cdot H_S(f, \theta) \tag{37}$$

and

$$H_S(f, 0^o) = H_s(f) \tag{38}$$

47

$H_s(f, \theta)$ is a complex factor involving both frequency and angle of incidence that is required to convert the pressure frequency response function to a free field frequency response function. Since the magnitude of $H_s(f, \theta)$ can vary over a range greater than 12 db (a factor of $\pm$ 4 in the SPL), it must be accurately known if accurate free field sound pressure level measurements are going to be made.

3.2 ENVIRONMENTAL INACCURACIES

The primary test laboratory environments causing inaccuracies in the performance of piezoelectric microphones can be separated into two categories - climatic and dynamic. The specific climatic environments are temperature and relative humidity. The dynamic environments are vibration and acoustics.

As with piezoelectric accelerometers, the sensitivity, internal capacitance, and shunt resistance of piezoelectric microphones vary with temperature. The resultant effects of a temperature variation is a change in both the over-all microphone system sensitivity and in the low frequency response. As previously discussed, the shunt capacitance of the microphone to signal conditioner cable will reduce the magnitude of these variations. Since the actual magnitudes of the variations are so strongly dependent on the transducer material and construction, one should select a microphone whose above parameters will not exceed the allowable error tolerances, or determine the variation of these parameters with temperature and then measure the temperature during the test and later correct the measurements.

Relative humidity does not directly effect the accuracy of piezo-electric microphones as the transducer material, though sensitive to humidity, is hermetically sealed. Condensation of moisture on the connectors can cause degradation of the low frequency response.

48

Contrails (watermark at top)

Vibration of piezoelectric microphones results in spurious outputs. In Figure 18a, the simplified mechanical diagram of a piezoelectric micro-phone is drawn. Application of pressure $[p(t)]$ to the mass (m) causes a relative displacement $y(t)$. This measure of $y(t)$ is the output of the microphone. Note in Figure 18b that the same mechanical system will also produce an output $[y(t)]$ when the foundation is excited with an acceleration $\ddot{x}(t)$.

(a) Mass Excitation   (b) Foundation Excitation
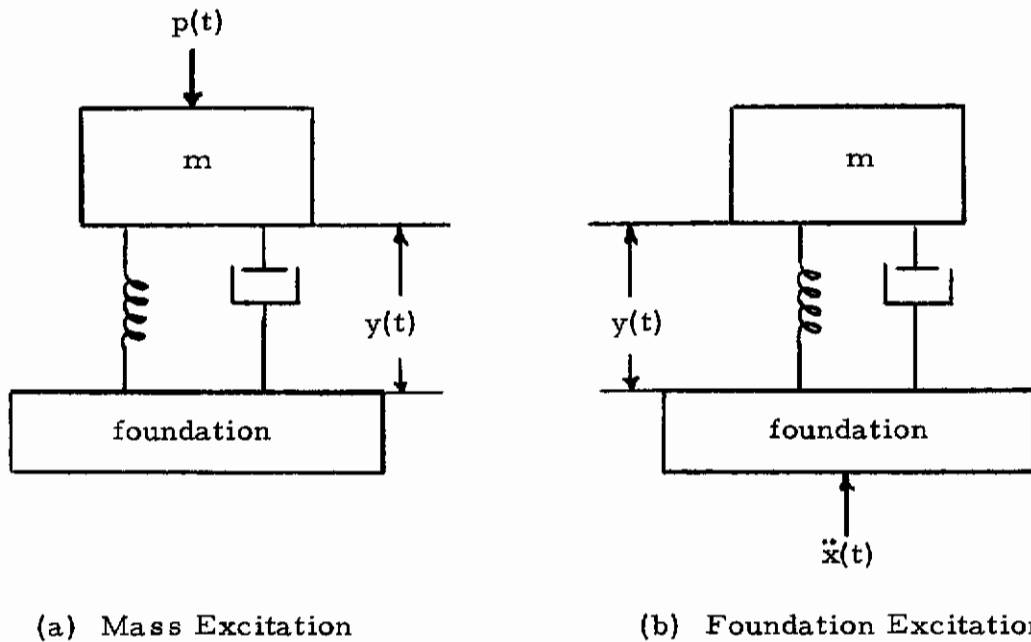
Figure 18. Simple Mechanical System Representation of a Microphone

Comparison of Eqs. (28) and (20), the equations of motion for Figure 18a and 18b, respectively, shows that the magnitude of the frequency response function for the microphone (18a) is essentially equal to the magnitude of the frequency response function of the accelerometer divided by a factor of $1/(2\pi f_n)^2$. Thus, if the undamped natural frequency of the microphone could physically be increased without decreasing its sensitivity,

49

Approved for Public Release

the spurious output due to vibration could be reduced. However, in the practical case, increasing the natural frequency means decreasing the mass (hence, sensitive area) and/or increasing the spring constant of the microphone. Both of these steps decrease the sensitivity of the microphone. To be more specific, the force applied to the mass in Figure 18a is

$$F_1 = p \frac{s}{k} \tag{39}$$

where

F_1 = the equivalent force applied to the mass of the microphone of
    Figure 18a in rms pounds

p = the acoustic pressure applied to the mass of the microphone
    in rms pounds per square inch

s = the sensitive area of the microphone system in square inches

k = the spring constant of the microphone in pounds per inch

For a given p, either the decrease of s or increase of k results in a decrease in F. Hence, the net result of increasing the natural frequency of a microphone may be an increase in the equivalent spurious acceleration response.

Techniques that have been used to minimize the response of microphones to vibration include both "soft" mounting and electrical subtraction of the vibrations. These techniques will be discussed further under the usage inaccuracy section.

Typical values (Ref. [27]) for the spurious output of piezoelectric microphones, in terms of equivalent SPL for a 1 g vibration, vary from 105 db to 145 db re .0002 μbar.

50

3.3   USAGE INACCURACIES

This category of inaccuracies is separated into two sections. The first section deals with inaccuracies related to physical conditions -- location, mounting, and size.   The second section discusses calibration inaccuracies.

3.3.1   Physical Problems

The relative importance of the size of the microphone depends upon the type of measurement desired.   For free field sound pressure level measurements, as discussed in Section 3.1, a very small microphone is desirable to minimize:

(1)   the difference between the free field and pressure response of the microphone at the upper range of measurement frequencies,

(2)   the disturbance to the sound field,

(3)   the dependence of the frequency response function upon the angle of incidence of the sound pressure upon the sensitive surface of the microphone.

For measurement of the sound pressure impinging upon a surface, as illustrated in Figure 19, the size of the microphone is not critical for the above reasons, and, in fact, the size has no effect upon the measurement accuracy if the entire surface is exposed to a uniform pressure distribution and if installation of the microphone does not alter the pressure distribution. In real life, it will frequently be found that there is a pressure gradient across the surface, and/or that the microphone installation disturbs the pressure field.   Use of a small microphone tends to reduce the magnitude of these problems.

p(t)
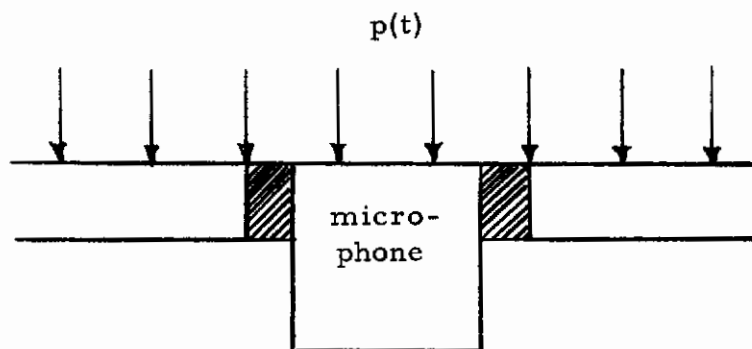
Figure 19. Measurement of Acoustic Pressure Impinging on a Surface

The proper location for any one microphone depends on many factors
such as:

(1)   the type of test; i. e., plane wave, standing wave, or reverberant

(2)   the type of measurement; i. e., free field SPL or pressure

(3)   the purpose of the measurement; i. e., environment certification,
response determination, absorptivity, etc.

It is impossible to specify the proper location criteria for every test, but
in general the following guidelines apply.

(1)   For plane wave tests, the microphone should be oriented so
that the angle of incidence is 0°. (For microphones with one
flat sensitive surface, this surface should be perpendicular to
the pressure wave.)

(2)   For free field environmental certification measurements, the
microphone should be sufficiently far away from the nearest
surface to avoid the effects of the pressure wave reflections.

Mounting of piezoelectric microphones is a problem primarily
because of their vibration susceptibility. Given a choice, one should
(1) select a microphone that is relatively insensitive to vibration,
(2) attach the microphone to a massive structure, and/or (3) attach the
microphone through a vibration isolator. These options should be taken
in the order stated.

52

Reduction of the vibration sensitivity of microphones by subtraction of an electrical signal equal to its spurious output due to vibration has proven quite effective. This is accomplished by building a piezoelectric accelerometer into the microphone. The electrical output of the piezo-electric crystal used for acoustic measurement is connected to the electrical output of the piezoelectric crystal used for acceleration measurements in such a manner that the electrical outputs subtract. When the microphone is vibrated, its output is the difference between these two signals. If the microphone is vibrated and the sound pressure is zero, as in a vacuum, the output is merely the difference between the vibration sensitivity of the two crystals. Theoretically, this could be made equal to zero if the two simple mechanical systems could be made identical.

Attaching the microphone to a massive structure so that there will be very little vibration of the microphone is rarely feasible. For free field measurements, the structure will distort the sound pressure field and for pressure measurements the structures that are generally of most interest are not massive.

Vibration isolation of microphones is frequently used. The purpose of the isolator is to reduce the acceleration level of the microphone and, in turn, the spurious output of the microphone. The isolators tend to increase the spurious acceleration response at low frequencies and tend to reduce this spurious response at high frequencies. The design of practical vibration isolators that both attenuate the vibration sensitivity of microphones over the entire band of frequencies likely to be encountered during acoustic testing and prohibit rotational motion is difficult. All vibration isolation systems for microphones should be empirically evaluated before they are used in order to verify that use of the isolation system is beneficial.

3.3.2 Calibration Inaccuracies

The accurate calibration of microphones over a wide frequency and amplitude range is quite difficult and time consuming. Therefore, selection of the calibration method that yields only the accuracy required for the particular measurement can result in considerable time savings.

Some of the more common calibration methods include:

(1) single amplitude, single frequency calibration (Pistonphone)

(2) reciprocity calibration

(3) electrostatic calibration

(4) free field substitution calibration

Calibration by use of pistonphone is very simple. The microphone is inserted into the pistonphone and a switch thrown, or a potentiometer adjusted to give a particular reading on a self-contained meter. The microphone is then subjected to whatever SPL the pistonphone is designed for. The calibration is usually only at one frequency and this frequency is usually between 100 and 1000 cps. The advertised accuracy for this type of calibrator ranges from $\pm$ .2 db ($\sim 2\%$ voltage error) to $\pm$ 1 db ($\sim {}^{+12}_{-11}\%$ of the output voltage).

Reciprocity calibration of either the free field or pressure response is possible. Pressure response calibration by reciprocity is far more common because this response function can be measured with a device costing several hundred dollars whereas reciprocity calibration of the free field response requires an anechoic chamber. Reciprocal calibration of the pressure response function is an absolute calibration and is the most accurate calibration that can be presently performed. Accuracies of $\pm$ .2 db ($\sim \pm 2\%$ of the output voltage) are possible. The frequency range over which this calibration can be accurately made is limited because the pressure distribution inside of the calibrator becomes uneven at high

54

frequencies. This type of calibration requires a fair amount of time to perform properly. (For details on this calibration method, see Refs. $\left[28, 29, 30\right]$.) Free field reciprocity calibration can be performed to an accuracy of $\sim \pm$ .5 db ($\sim \pm$ 6% of the output voltage).

Electrostatic calibration is a commonly employed method for determining the frequency response of microphones. The microphone is inserted into a device that generates an electrostatic force on the sensitive surface of the microphone. This force creates a motion of the sensitive surface of the microphone that simulates motion due to sound pressure. These devices can simulate a constant pressure level over frequency ranges up to 200 kc. Their advertised accuracy for absolute calibration is $\pm$ 1.5 db ($^{+19}_{-16}$% of the output voltage). These devices are frequently used to measure the relative response at different frequencies where the absolute sensitivity has been determined by another calibration method.

Free field substitution or comparison calibration is quite similar to back-to-back calibration of accelerometers, but is considerably more difficult to perform. A microphone that is calibrated by NBS is exposed to a sound pressure level in a free field and its output voltage is measured. The calibration, or standard, microphone is then replaced by the microphone to be calibrated and its output is measured. The sensitivity of this microphone is then the ratio of its output voltage to the output voltage of the standard microphone times the sensitivity of the standard microphone. Care must be taken to assure that both microphones are subjected to the same SPL.

If possible, it is desirable to perform a simple calibration (pistonphone) prior to and following each test to check for gross errors and transducer system failures. It is also desirable to periodically perform a thorough calibration of each microphone to check for sensitivity drift.

55

One of the practical problems that may occur in calibration is that the calibration devices are generally designed for one particular microphone and microphones with different dimensions cannot be calibrated. Adapters can be built, but they must be carefully designed and usually reduce the calibration accuracy.

56

4. STRAIN MEASURING SYSTEMS

At the present time variable resistance strain gages are used to a far greater extent for the measurement of dynamic strain than any other type of transducer. These variable resistance strain gages are available in unbonded or bonded forms. Unbonded strain gages are constructed as shown in Figure 20.
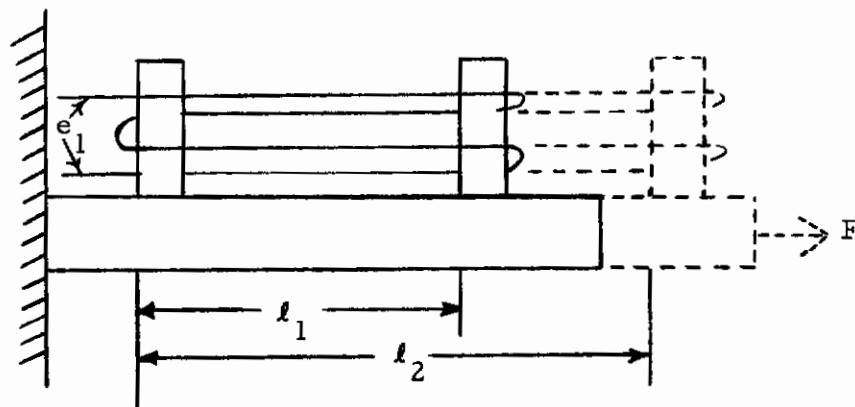
Figure 20. Construction of an Unbonded Strain Gage

A wire or other resistance material is attached rigidly to the electrically insulated posts. When a load, F, is applied as shown above, the length of the specimen being measured increases from ℓ_1 to ℓ_2. The unit deformation, or unit strain, is:

$$\epsilon = \frac{\ell_2 - \ell_1}{\ell_1} = \frac{\Delta \ell}{\ell_1} \tag{40}$$

where

ϵ = the unit deformation (unit strain) of the test specimen

ℓ_1 = the zero strain length of the test specimen in inches between the posts before the force is applied

57

ℓ_2 = the length of the test specimen in inches between the posts after the force F is applied

$\Delta\ell$ = the change in the length of the test specimen in inches between the posts due to the applied force F

F = the applied force in pounds

Since the posts are rigidly attached to the test specimen, the resistance element of the strain gage will be subjected to the same unit deformation as the test specimen. Assume that when the force is applied in the direction shown in Figure 20, the resistance of the strain gage will increase.

$$R_{g_2} - R_{g_1} = \Delta R_g \qquad (41)$$

where

R_{g_1} = the resistance of the resistance element of the strain gage in ohms before the force is applied

R_{g_2} = the resistance of the resistance element of the strain gage in ohms after the force F is applied

ΔR_g = the change of resistance in ohms of the strain gage due to the change in length of the test specimen

As long as it is proportional to the change in length of the test specimen, the change in resistance of the strain gage provides a convenient method for measuring this change in length. The proportionality of the resistance change to the unit deformation is usually expressed as follows:

$$\frac{\Delta R_g}{R_{g_1}} = K \frac{\Delta\ell}{\ell_1} = K\epsilon \qquad (42)$$

$$K = \frac{\dfrac{\Delta R_g}{R_{g_1}}}{\dfrac{\Delta\ell}{\ell_1}} \qquad (43)$$

58

where K is the dimensionless "gage factor" or sensitivity of the strain
gage.

Bonded filament strain gages normally have their resistance element,
or filament, attached to a thin layer of insulation called a carrier. The major
purposes of the carrier are to electrically insulate the resistance element
of the strain gage from the test specimen and to facilitate bonding of the
strain gage to the test specimen. The operating principle of the bonded
filament strain gage is identical to that of the unbonded strain gage. Because
the bonded gages are so convenient to use and because they are available
with a very wide variety of resistance materials, carrier materials, and
configurations designed for special applications, these gages are quite
popular.

Other types of transducers for the direct measurement of dynamic
strain include variable inductance strain gages, variable capacitance strain
gages, and acoustic, or taut wire strain gages. Dynamic strain can some-
times be measured indirectly by the use of displacement, velocity, and
acceleration transducers. See Ref. [4]. Since the bonded filament type
of strain gages will be used for strain measurements in the Sonic Fatigue
Facility, the remainder of the discussions in Section 4 will be restricted to
this category of strain gage.

To detect this change in resistance, an electrical excitation of the
strain gage is required. This excitation may be either AC or DC.   AC
excitation has the advantage of requiring less DC stability of the signal
conditioner for measurement of static strains. Since the voltage out of
practical strain gage systems is likely to be in the order of a few millivolts,
this is an important advantage. With AC excitation, these millivolts can be
amplified to relatively large voltage levels with AC amplifiers so that only
the demodulator and the output stage of the signal conditioner are required
to have low DC drift. Since these two stages are operating at relatively high

59

voltage levels, it is not difficult to design the required drift stability into these stages. While the use of DC excitation requires signal conditioners with extremely low drift characteristics (hence, expensive signal conditioners), DC excitation does eliminate the reactive unbalance problem encountered with AC excitation; and this could be a serious problem with cables as long as those at the Sonic Fatigue Facility. Because DC excitation is used in this facility, further discussions will be restricted to this category.

4.1 POTENTIOMETER CIRCUIT

Normally the strain gage is used as either a leg of a potentiometer circuit or as a leg of a bridge circuit. Figure 21 shows a strain gage used in a typical potentiometer circuit.
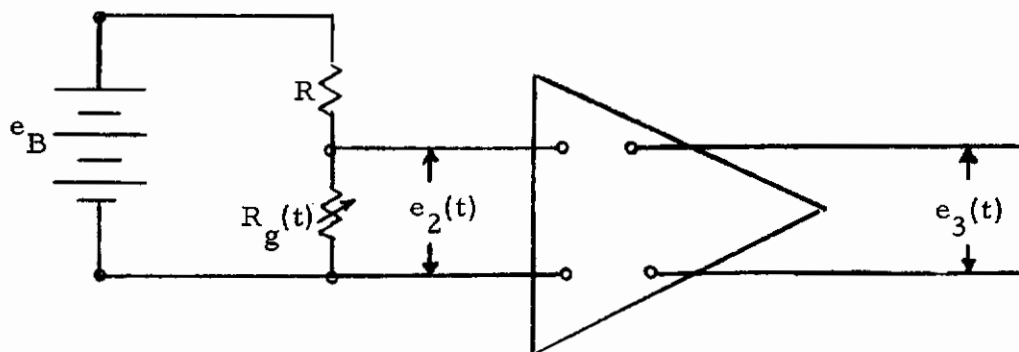
Figure 21. Variable Resistance Strain Gage
Used in a Potentiometer Circuit

The voltage across the strain gage is:

$$e_2(t) = \frac{e_B R_g(t)}{R + R_g(t)} \tag{44}$$

60

where

$e_2(t)$ = the instantaneous voltage at the input to the amplifier section of the signal conditioner

e_B = the excitation in volts DC

R = the resistance of the bleeder resistor in ohms

$R_g(t)$ = the instantaneous resistance of the strain gage in ohms

Figure 22a shows a time history of a variation in length of a strain gage bonded to a test specimen, and Figure 22b shows the time history of the corresponding change in resistance of this strain gage attached to the test specimen.

Figure 22a. Plot of $\ell(t)$
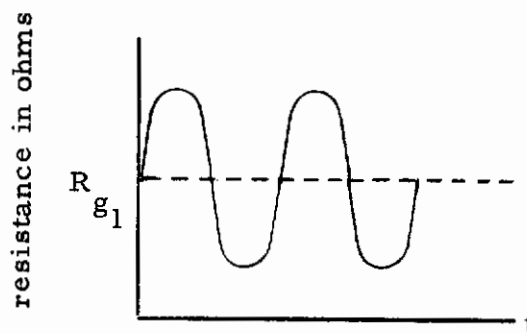
Figure 22b. Plot of $R_g(t)$ Corresponding to $\ell(t)$

From Eq. (42),

$$\epsilon = \frac{\Delta \ell}{\ell_1} \quad \text{and} \quad K\epsilon = \frac{\Delta R_g}{R_{g_1}}$$

hence,

$$\epsilon(t) = \frac{\ell(t) - \ell_1}{\ell_1} \tag{45}$$

61

and

$$K\epsilon(t) = \frac{R_g(t) - R_{g_1}}{R_{g_1}} \tag{46}$$

$$R_g(t) = R_{g_1}\left[1 + K\epsilon(t)\right] \tag{47}$$

where

$\epsilon(t)$ = the instantaneous unit deformation, or strain

$\ell(t)$ = the instantaneous length of the strain gage in inches

ℓ_1 = the unstrained length of the strain gage in inches

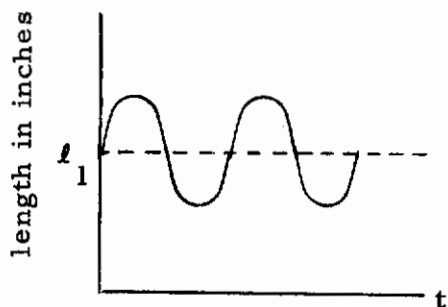$R_g(t)$ = the instantaneous resistance of the strain gage in ohms

R_{g_1} = the unstrained resistance of the strain gage in ohms

By combining Eqs. (44) and (47), it is possible to solve for $e_2(t)$ in terms of $\epsilon(t)$

$$e_2(t) = \frac{e_B\left[1 + K\epsilon(t)\right]}{\left(\dfrac{R}{R_{g_1}} + 1\right) + K\epsilon(t)} \tag{48}$$

If only the dynamic strain is of interest, it can be found by subtracting $e_2(0)$, the quiescent (unstrained) value of the strain gage output voltage, from $e_2(t)$, as follows.

$$e_2(t) - e_2(0) = e_B\left[\frac{1 + K\epsilon(t)}{\left(\dfrac{R}{R_{g_1}} + 1\right) + K\epsilon(t)} - \frac{1}{\dfrac{R}{R_{g_1}} + 1}\right] \tag{49}$$

Usually this is the case as the quiescent voltage is generally much greater than the dynamic voltage $e_2(0) >> \left[e_2(t) - e_2(0)\right]$. Physically, the removal of the quiescent voltage can be accomplished by installing a blocking

62

capacitor between the output of the strain gage and the input of the signal conditioner.

From Eqs. (48) and (49), it is readily apparent that the voltage out of the strain gage is not a linear function of strain. Rearranging Eq. (49),

$$e_2(t) - e_2(0) = \frac{\left(\dfrac{R}{R_{g_1}}\right) e_B K \epsilon(t)}{\left(\dfrac{R}{R_{g_1}} + 1\right)^2 + K \epsilon(t) \left(\dfrac{R}{R_{g_1}} + 1\right)} \qquad (50)$$

It should be noted that the $K \epsilon(t) \left(\dfrac{R}{R_{g_1}} + 1\right)$ term in the denominator of Eq. (50) is frequently omitted in the literature so that the voltage out of the strain gage appears to be linear. The resulting percentage error from making this simplifying assumption is

$$\% \text{ error} = \frac{(100) K \epsilon(t)}{\dfrac{R}{R_{g_1}} + 1} \qquad (51)$$

Since the ratio of R/R_{g_1} is usually made near to unity $\left(\text{see Ref. } [31] \right)$ to maximize the dynamic voltage for a given power supply voltage, the percent error can become quite appreciable at either high gage factors or high strains.

The voltage could have been measured across the bleeder resistor instead of the strain gage. For this case, the equivalent of Eq. (44) is

$$e_2(t) = \frac{e_B (R)}{R + R_g(t)} \qquad (52)$$

63

and the dynamic voltage equivalent of Eq. (50) is

$$e_2(t) \div e_2(0) = \frac{-\left(\dfrac{R}{R_{g_1}}\right)(K)\left[\epsilon(t)\right]\left(e_B\right)}{\left(\dfrac{R}{R_{g_1}} + 1\right)^2 + \left(\dfrac{R}{R_{g_1}} + 1\right) K\epsilon(t)} \qquad (53)$$

4.2 WHEATSTONE BRIDGE CIRCUIT

Wheatstone bridge circuits are also used with variable resistance strain gages. In fact, they are probably used more frequently than the potentiometer circuit. The main advantage of the Wheatstone bridge circuit over the potentiometer circuit is that the quiescent voltage can be balanced out. The main disadvantage is that the ground of the excitation power supply and the ground of the signal conditioner must be electrically isolated. Figure 23 shows a strain gage used in a typical Wheatstone bridge circuit.
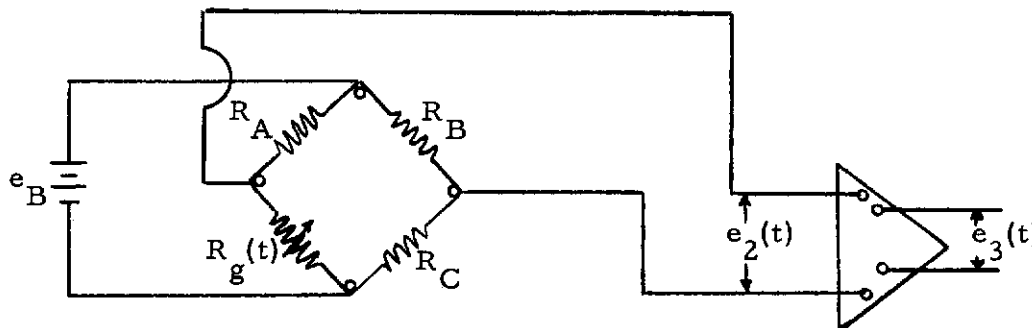
Figure 23. Variable Resistance Strain Gage
Used in a Wheatstone Bridge Circuit

If one assumes that all of the arms of the bridge have an equal resistance of R at t = 0, the excitation supply has zero source impedance, and the

64

signal conditioner has infinite input impedance, the simplified equivalent circuit diagram of Figure 23 can be drawn as shown in Figure 24.
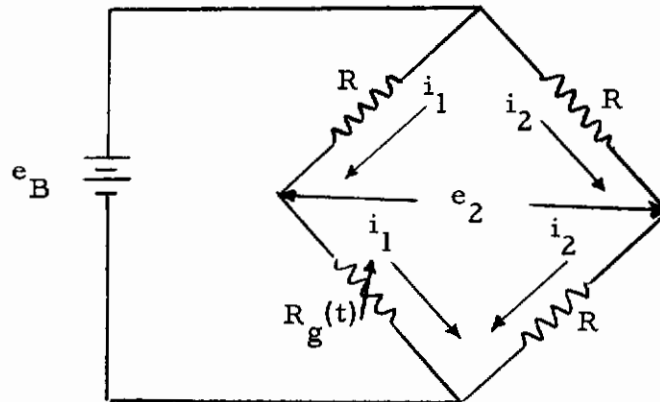
Figure 24.   Simplified Equivalent Circuit of a Wheatstone Bridge

The output voltage can be found as follows

$$e_2 = i_2 R - i_1 R = R(i_2 - i_1) \tag{54}$$

where

$$i_2 = \frac{e_B}{R + R} = \frac{e_B}{2R}$$

$$i_1 = \frac{e_B}{R + R_g(t)} = \frac{e_B}{2R} \text{ at } t = 0, \text{ since } R_g(0) = R_{g_1} = R$$

$$\therefore e_2 = 0$$

which simply states that the bridge is balanced. By combining Eqs. (54) and (47), one can solve for $e_2(t)$ for this special case.

65

$$e_2(t) = (e_B)(R)\left(\frac{1}{2R} - \frac{1}{R + R_g(t)}\right)$$

$$e_2(t) = (e_B)(R)\left(\frac{1}{2R} - \frac{1}{R + R_{g_1} + R_{g_1} K\epsilon(t)}\right)$$

$$R_{g_1} = R \text{ for this special case}$$

$$e_2(t) = \frac{e_B\left[K\epsilon(t)\right]}{4 + 2K\epsilon(t)} \tag{55}$$

Thus, it can be seen that the output of the Wheatstone bridge is not a linear function of strain. Frequently the $2K\epsilon(t)$ term in the denominator is omitted so that output of the bridge appears to be a linear function of strain. The percent error from making this assumption is

$$\% \text{ error} = \left[\frac{K\epsilon(t)}{2}\right](100) \tag{56}$$

Whenever both the gage factor and the strain are quite low, the error will be negligible. However, wherever the gage factor, or the strain is high, the error will be quite appreciable.

Because the Wheatstone bridge circuit configuration will be used for strain measurements in the Sonic Fatigue Facility, further discussions shall be limited to this arrangement. More general equations for the operation of the Wheatstone bridge will be presented under the discussion of intrinsic inaccuracies.

For clarity, the discussions of the bridge and excitation circuits will be separated from the discussions of the remainder of the signal conditioner circuitry. For the remaining portion of the signal conditioner circuitry, only the differences from the details presented in Section 2 will

66

be discussed because these circuits are identical except that the impedance converter (cathode follower) is not used for strain measurements.

4.3 INTRINSIC INACCURACIES

The intrinsic inaccuracies of strain measuring systems can be broken down into inaccuracies due to:

(1) Deviations from the theoretical frequency response function due to the amplitude of the applied strain;

(2) deviations from the theoretical frequency response function due to the frequency of the applied strain; and,

(3) transverse sensitivity.

Figure 25 shows the basic block diagram of a strain gage system where the strain gage is separated from the remainder of the bridge circuit by a long cable, such as in the Sonic Fatigue Facility.
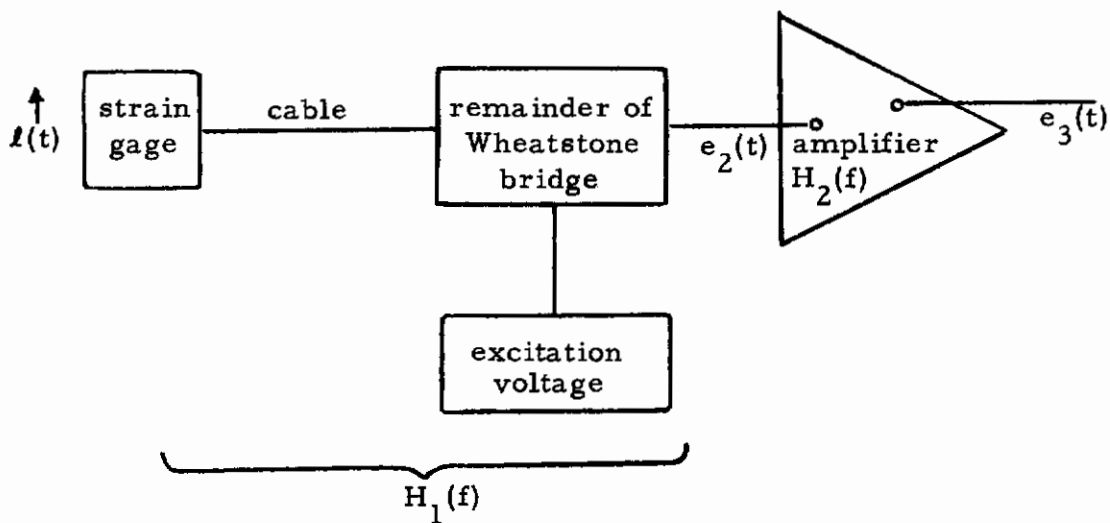
Figure 25. Basic Block Diagram of a Strain Measuring System

67

The "ideal" frequency response functions (see Ref. $\left[12\right]$) for $H_1(f)$ and $H_2(f)$ would be constants as given by

$$H_1(f) = K_1$$

$$H_2(f) = K_3 + \frac{e_D}{e_2(t)}$$

where

$H_1(f)$ = the frequency response function between $e_2(t)$ and $\ell(t)$ for given bridge resistance and excitation voltage values, in volts

$H_2(f)$ = the dimensionless frequency response function between $e_2(t)$ and $e_3(t)$

$e_2(t)$ = the instantaneous value of the voltage at the input to the amplifier stage of the signal conditioner

$e_3(t)$ = the instantaneous value of the voltage at the output of the signal conditioner

e_D = the DC drift or bias voltage on the output of the signal conditioner

K_1 = the dimensionless gage factor of the strain gage

K_3 = the signal conditioner gain (dimensionless)

$\ell(t)$ = the instantaneous value of the length of the strain gage in inches

ℓ_1 = the unstrained length of the strain gage in inches

4.3.1 Strain Gage

The amplitude linearity characteristics of variable resistance bonded strain gages (the variation of K_1 as a function of $\left[\ell(t) - \ell_1\right]/\ell_1$) are quite good when the gages are used at strain amplitudes below their rated maximum levels. The nonlinearity of strain gages (and their bonding material) is frequently expressed in terms of the hysteresis occurring after the gage has been subjected to three load cycles. See Figure 26.

68
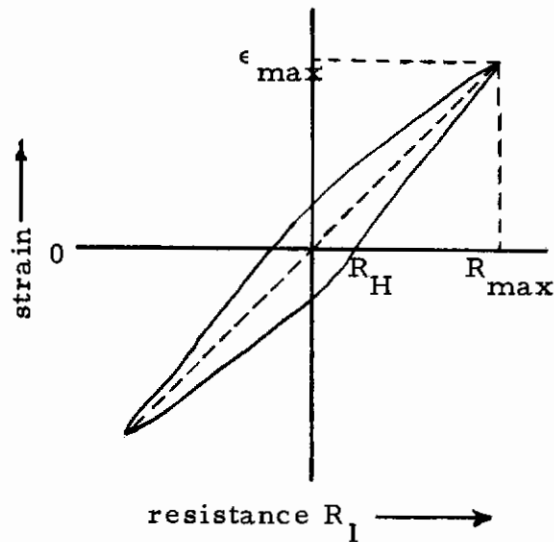
Figure 26.   Illustration of Strain Gage Hysteresis

The percent hysteresis is

$$\%N = (100)\ \frac{R_H - R_{g_1}}{R_{max} - R_{g_1}} \tag{57}$$

where

$\%N$ = the hysteresis expressed in percentage of full scale

R_{max} = the resistance in ohms of the strain gage corresponding to full scale strain

R_{g_1} = the resistance of the resistance element of the strain gage in ohms before the force is applied

R_H = the resistance in ohms of the strain gage at no load after three complete cycles of plus and minus full scale strain

ϵ_{max} = the full scale strain

References [32, 33, 34] summarize the results of linearity measurements on several types of strain gages. References [35, 36] summarize the results of tests to measure the contribution of the bonding cement to hysteresis and Ref. [37] summarizes the results of tests to measure the linearity of strain gages at high strain magnitudes. All of these references quote hysteresis error of less than $\pm$ 1% of full scale.

69

One problem related to amplitude nonlinearity that has not yet been well-defined is the degradation in performance of these gages when they are used to measure the fatigue life of a test specimen. Since the strain gages are mechanical devices, it is reasonable to expect that they will have a finite fatigue life. Reference [38], a summary of the present knowledge of the fatigue life of strain gages, concludes that present day knowledge is insufficient to state whether strain gages will even "outlive" the structures to which they are attached in sonic fatigue tests. Hence, it appears that additional research in the form of a carefully planned test program should be performed to determine both the life and degradation in accuracy of strain gages as a function of stress magnitude and duration (S-N type curves to a certain percent inaccuracy and to failure).

Another amplitude related inaccuracy that occurs in certain types of strain gages is due to the self-generating characteristics of some of the materials used for the strain sensitive resistance element. This effect occurs only when the resistance materials are magnetic and is called magnetostriction. The actual voltage generated is a function of the resistance material, the current through the gage, the frequency of strain, and the amplitude of the strain. This magnetostrictive effect can cause two types of intrinsic errors. First, an output voltage will be obtained from gages that exhibit this effect even when no excitation voltage is applied to the gage. Second, the ideal gage factor, K_1, is altered by the addition of a voltage in series with the normal voltage across the strain gage. See Figure 27.
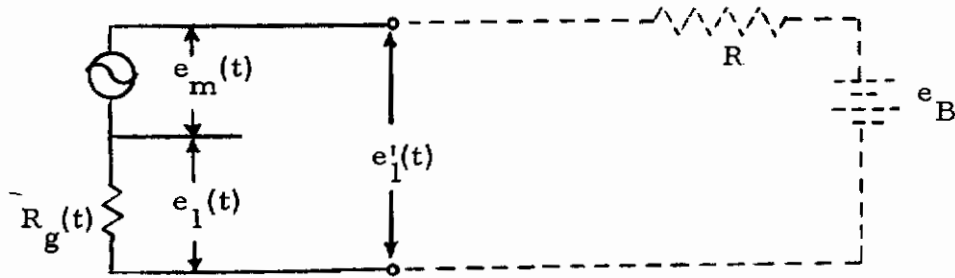
Figure 27. Illustration of the Change in Gage Factor
Due to Magnetostriction

$$e_1'(t) = e_1(t) + e_m(t) \tag{58}$$

where

$e_1'(t)$ = the total instantaneous voltage developed across the strain gage

$e_m(t)$ = the instantaneous voltage developed by the magnetostrictive
    effect

The ideal gage factor is

$$K_1 = \frac{\left(R_g(t) - R_{g_1}\right)\Big/ R_{g_1}}{\left(\ell(t) - \ell_1\right)\Big/ \ell_1} \tag{59}$$

The effective resistance, R_{eff}, of the strain gage (including the magneto-
strictive effects) is

$$R_{eff}(t) = \left[\frac{R + R_g(t)}{1 - \dfrac{e_m(t)}{e_B}}\right] - R \tag{60}$$

where R equals the resistance in ohms of the bridge leg in series with the
strain gage (between the terminals of the excitation voltage). The effective
gage factor, $K_{1(eff)}$, is

71

$$K_{1(eff)} = \frac{\left[R_{eff}(t) - R_{g_1}\right]/R_{g_1}}{\left(\ell(t) - \ell_1\right)/\ell_1} \tag{61}$$

Obviously, if $e_m(t)/e_B$ is very small, the resulting error due to magneto-striction will be small. Since the magnitude of $e_m(t)$ is so strongly dependent on the gage construction, its value should be determined for any strain gage before it is used for quantitative measurements. For further discussions of magnetostriction, see Refs. [39, 40].

For a strain gage of reasonable dimensions that is constructed of non-magnetic materials, K_1 could be considered to be independent of frequency (over a 0 to 10 kc frequency range). As discussed in the preceding paragraph, the apparent gage factor is a function of frequency for strain gages that exhibit the magnetostrictive effect. The primary variation of K_1 with frequency is due to being bonded to a real structure. Because the strain gage has finite area, its output will be proportional to the mean strain developed over the area of the strain gage.

Reference [39] develops an equation relating the mean strain over the surface of a strain gage to the strain at the midpoint of the gage. This equation is

$$\frac{\epsilon}{\epsilon_0} = \frac{\sin \dfrac{\pi \ell_1}{\lambda}}{\dfrac{\pi \ell_1}{\lambda}} \tag{62}$$

where

ϵ = the mean strain over the length of the strain gage

ϵ_0 = the strain at the midpoint of the strain gage

ℓ_1 = the unstrained length of the strain gage in inches

λ = the propagation wave length in the test specimen in inches per cycle

72

The above equation applies for either longitudinal or bending strains. One can either set the allowable error and solve for the corresponding frequency, or set the highest strain frequency and solve for the corresponding error.

$$f = \frac{\lambda}{c} \qquad (63)$$

where

f = the strain frequency in cycles per second

c = the velocity of propagation in the test specimen in inches per second

The important points are:

(1) The apparent gage factor will be dependent upon the frequency of strain.

(2) The specific variation in apparent gage factor as a function of frequency is dependent upon the length of the strain gage and the structural characteristics of the test specimen.

(3) The maximum allowable frequency for a given percent error will increase as the gage length decreases (linearly for longitudinal strains and by the second power for bending strains).

(4) The error corresponding to the highest expected strain frequency should always be calculated for each strain gage installation.

Because the majority of commercial strain gages are presently designed with the resistance element shaped in some sort of grid to obtain a reasonably high resistance value in a relatively short gage length, some of the resistance element must be oriented non-parallel to the sensitive axis of the strain gage. This results in a spurious response of the strain gage to transverse strains. The indicated strain will be the sum of the strain in the sensitive direction and a percentage of the strain in the transverse direction.

73

$$\epsilon'(t) = \epsilon(t) + \frac{\xi}{100} \epsilon_T(t) \qquad (64)$$

where

$\epsilon'(t)$ = the total indicated instantaneous strain

$\epsilon_T(t)$ = the instantaneous strain transverse to the sensitive axis of the strain gage

ξ = the percent response of the strain gage to transverse strains

The percent error in the measurement of strain along the sensitive axis is

$$\% \text{ error} = \xi \frac{\epsilon_T}{\epsilon} \qquad (65)$$

where

ϵ_T = the rms strain transverse to the sensitive axis of the strain gage

ϵ = the true rms strain along the sensitive axis of the strain gage

Obviously, strain gages with low transverse sensitivities (ξ) should be chosen for sonic fatigue measurements.

4.3.2 Cabling

Three wire shielded cable is used at the Sonic Fatigue Facility between the output of each strain gage and the input to its signal conditioner. This type of cabling permits the installation of one or two arms of the bridge on the test specimen in a manner that balances out the changes in resistance of the cable due to temperature variations. Consider the one active arm bridge as arranged in Figure 28. For simplicity, the fixed resistances are set equal to each other and to $R_g(t)$ at t = 0, although this is not necessary. The voltage drop across R_{L_2} (the resistance of the cable as shown below) can be ignored because the input impedance of the signal conditioners at the Sonic Fatigue Facility is very much greater than the sum of the bridge output resistance and R_{L_2}.

74
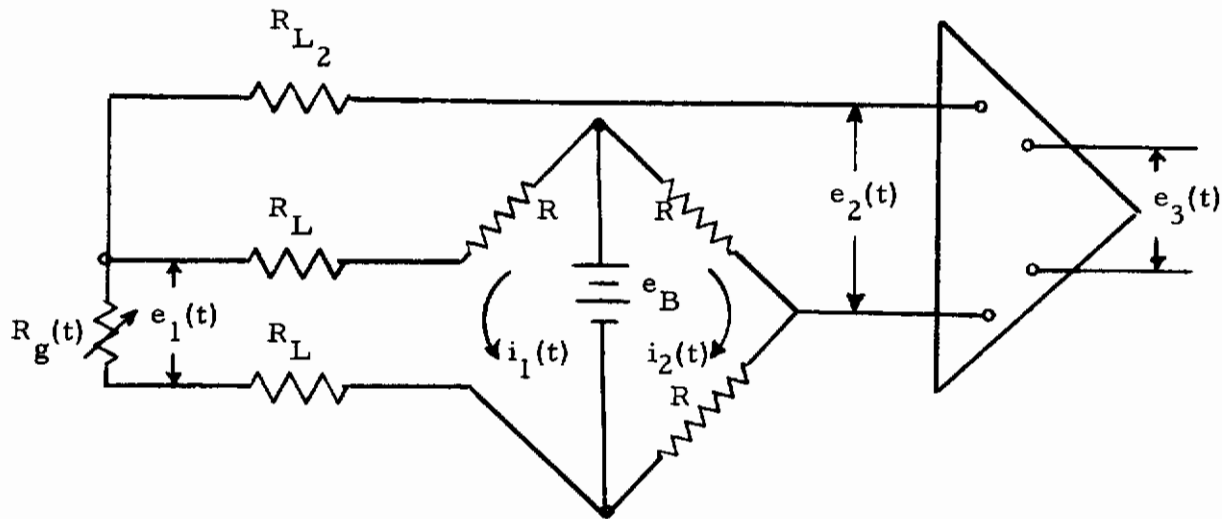
Figure 28. Three Wire Connection for a One Active Arm Wheatstone Bridge

Then, solving for the effect of the cable resistance (R_L's) in a form comparable to Eq. (55)

$$e_2(t) = e_B \left[\frac{K_1 \epsilon(t)}{\left(4 + 4\frac{R_L}{R}\right) + 2K\epsilon(t)} \right] \qquad (66)$$

For small strains and low gage factors, the cable resistances modify the magnitude of the frequency response function between $\epsilon(t)$ and $e_2(t)$, as described in Eq. (55), by a gain of approximately

$$\text{gain} \approx \frac{R}{R + R_L} \qquad (67)$$

To illustrate the magnitude of the error due to cable resistance, assume that all of the bridge resistances are 120 ohms, that the cable is 100 feet long, and the cable is constructed of No. 22 gage wire. For this example,

$$R_L = 100 \text{ ft} \times .016 \text{ ohms/ft} = 1.6 \text{ ohms}$$

$$\text{gain} = \frac{120}{120 + 1.6} = .987$$

Or, stated another way, the value of voltage at the input to the signal conditioner is reduced about 1.3% for a given strain when the strain gage is connected through the above cables.

Next, it is of concern to determine if the cable between the strain gage and the signal conditioner affects the frequency response of the system. The equivalent circuit of the Wheatstone bridge including the cable impedance is shown in Figure 29. (The insulation resistance is assumed to be sufficiently high so that shunt conductance can be ignored. Also, since the maximum strain frequency is only 10 kc and the length of the cable from the strain gage to the signal conditioner is only approximately 100 feet, the equivalent π section representation of this cable has been changed to lump all of the shunt capacitances at the transducer end of the cable.)
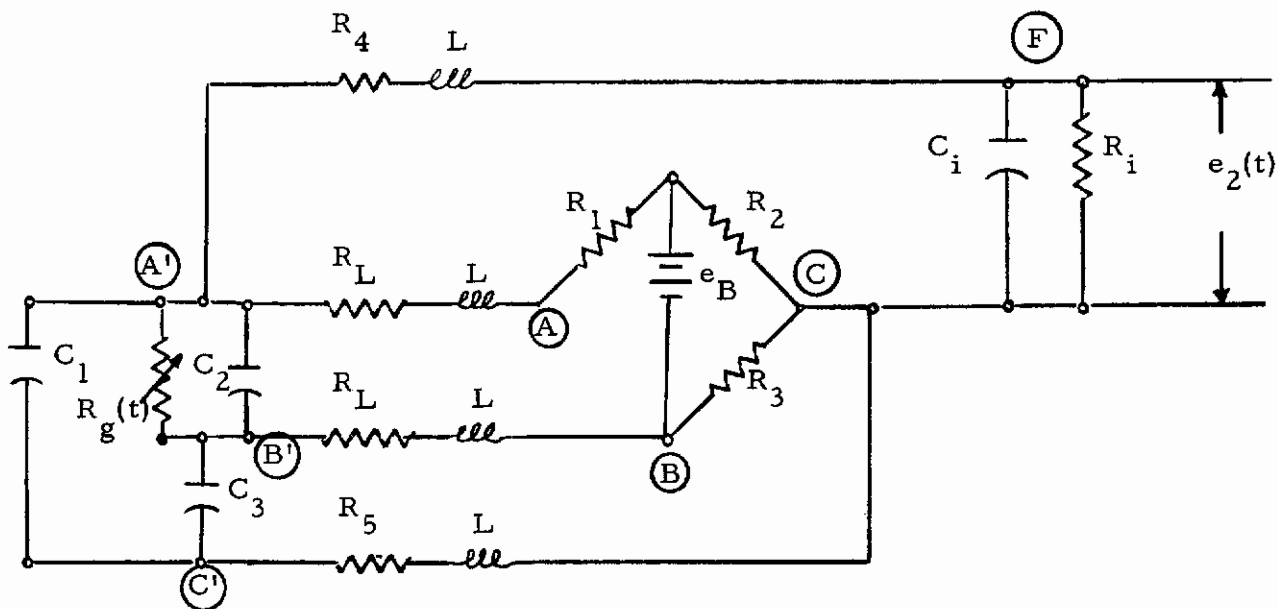

Figure 29. Equivalent Circuit of a Wheatstone Bridge
Including Parasitic Effects of the Trans-
ducer to Signal Conditioner Cable

R_1, R_2, R_3 = fixed bridge resistors

R_L = series resistance of the strain gage to bridge wires

R_4 = series resistance of the strain gage to signal conditioner wire

R_5 = series resistance of the cable shield

R_i = input resistance of the signal conditioner amplifier

L = series inductance of each wire in the cable

C_i = input capacitance of the signal conditioner amplifier

C_1 = sum of the shunt capacitances between the shield, ⓒ' to ⓒ, and both the wire from Ⓐ' to Ⓕ and the wire from Ⓐ' to Ⓐ

C_2 = sum of the shunt capacitances between the wire from Ⓑ' to Ⓑ and both the wire from Ⓐ' to Ⓐ and the wire from Ⓐ' to Ⓕ

C_3 = the shunt capacitance between the wire from Ⓑ' to Ⓑ and the shield ⓒ' to ⓒ

To study the effect of the parasitic impedances of the cable on the frequency response function between the applied strain and the input to the amplifier stage of the signal conditioner, conservative values for these impedances will be assumed and their effects determined individually. $\left[e_2(t) \right.$ could be determined by use of matrices, but the contributions of the individual impedances would then become obscured. $\left. \right]$

Assume

$$R_g(t) \text{ at } t = 0 = 120 \text{ ohms}$$
$$R_1 = R_2 = R_3 = 120 \text{ ohms}$$
$$R_L = 1.6 \text{ ohms}$$
$$R_4 = 5 \text{ ohms}$$
$$R_5 = 2 \text{ ohms}$$
$$R_i = 100 \text{ kilohms}$$

77

$$L = 0.2 \text{ microhenries/foot}$$

$$C_i = 50 \text{ picofarads}$$

$$C_1 = C_2 = C_3 = 50 \text{ picofarads/foot}$$

First, consider the effect of C_3, R_5, and L on the performance of the Wheatstone bridge. If their minimum impedance (Z_1) can be shown to be much greater than R_3, then the shunting effect of $X_{C_3} + R_5 + X_L$ across R_3 can be neglected (X_C and X_L are reactance values in ohms). The minimum impedance of Z_1 will occur at the highest frequency of operation (10 kc).

$$X_{C_3} = \frac{-j}{(2\pi)(10^4)(50 \times 10^{-12})(100)}$$

$$\approx -j \, 3.2 \times 10^3 \text{ ohms}$$

$$X_L = j2\pi fL = j(2\pi)(10^4)(.2 \times 10^{-6})(100) = j \, 1.3 \text{ ohms}$$

$$Z_1 = X_{C_3} + X_L + R_5 \approx -j \, 3.2 \times 10^3$$

To simplify the study of the effects of the above impedance in parallel with R_3, assume for the moment that the impedance between ⓑ' and Ⓑ equals zero. Then the impedance between Ⓑ and Ⓒ in this branch of the bridge is

$$Z_{\text{ⒷⒸ}} = \frac{Z_1 R_3}{Z_1 + R_3} = \frac{(-j \, 3.2 \times 10^3)(120)}{-j \, 3.2 \times 10^3 + 120} \approx 120 \text{ ohms } \angle 0^\circ$$

Thus, the effect of Z_1 in parallel with R_3 can be neglected.

Next, consider the effect of C_1, C_2, and C_3 on $R_g(t)$. Since $R_g(t)$ will only vary slightly from $R_g(0)$, its value will be assumed to be constant at 120 ohms.

78

$$Z_{\widehat{A'B}} = \frac{R_g(t) Z_2}{R_g(t) + Z_2}$$

$$Z_2 = \frac{\left(X_{C_2}\right)\left(X_{C_1} + X_{C_3}\right)}{X_{C_1} + X_{C_2} + X_{C_3}}$$

Z_2 will be a minimum at the highest frequency of operation; therefore, its value at 10 kc is

$$Z_2 = (-j)\left[\frac{1}{(2\pi)(10^4)(50 \times 10^{-12})(100)}\right]\left(\frac{2}{3}\right)$$

$$Z_2 = -j\, 2.1 \times 10^3$$

$$Z_{\widehat{A'B'}} = \frac{(120)(-j\, 2.1 \times 10^3)}{120 - j\, 2.1 \times 10^3} \approx 120 \text{ ohms } \underline{/0^\circ}$$

Therefore, the effect of the capacitances in parallel with $R_g(t)$ can be neglected, and the simplified circuit diagram can be redrawn as shown in Figure 30.
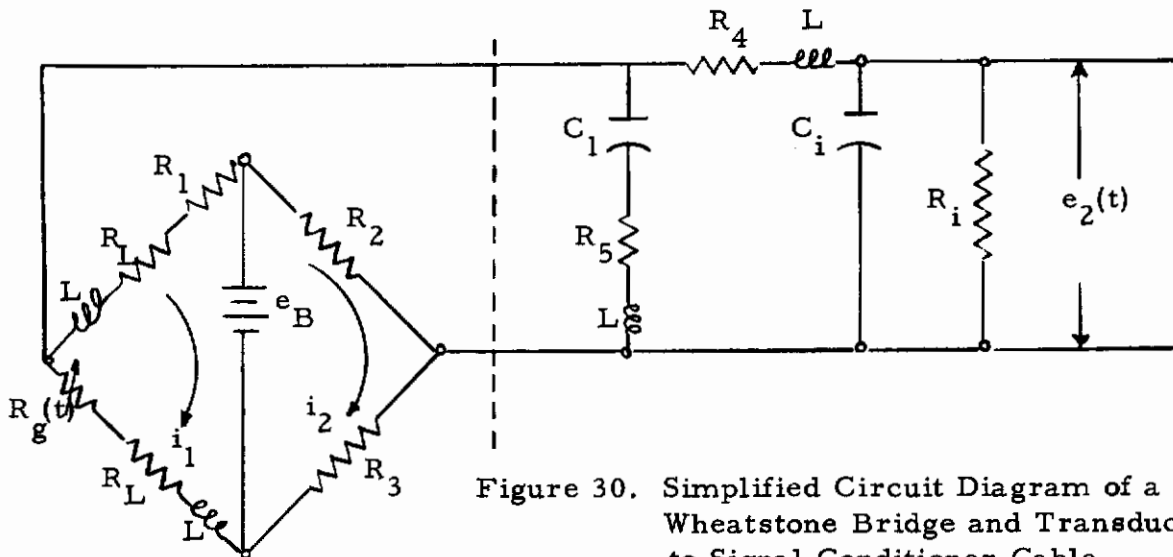
Figure 30. Simplified Circuit Diagram of a Wheatstone Bridge and Transducer to Signal Conditioner Cable

79

The effects of the remaining parasitic impedance will be studied by replacing the circuitry in Figure 30 left of the dotted line with an equivalent voltage generator $e_0(t)$ and output impedance Z_0 (Thévinin's Theorem) as shown in Figure 31.
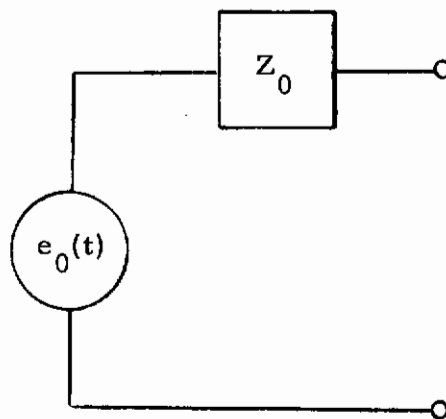
Figure 31. Replacement of Wheatstone Bridge by Equivalent Voltage and Impedance

Since the effect of the cable resistance was demonstrated in Eqs. (66) and (67), it will be assumed to be zero to determine the effects of series inductance in the transducer to bridge wires. Since the series impedance of the inductance will be greatest at the maximum frequency of operation, 10 kc, its effect will be investigated at this frequency.

$$e_0(t) = i_1 (R_1 + jX_L) + i_2 R_2$$

$$= i_1 \left[120 + j(2\pi)(10^4)(.2 \times 10^{-6})(100) \right] + i_2(120)$$

$$i_1 = \frac{-e_B}{\left[R_1 + R_g(t) \right] + j(2X_L)} = \frac{-e_B}{\left[240 + 120K_1 \epsilon(t) \right] + j(2)(2\pi)(10^4)(.2 \times 10^{-6})(100)}$$

$$i_2 = \frac{e_B}{R_2 + R_3} = \frac{e_B}{240}$$

$$e_0(t) = e_B = \left[\frac{K_1 \, \epsilon(t)}{\left[4 + 2K_1 \, \epsilon(t)\right] + j \, 0.042} \right]$$

Thus the cable inductance can be neglected and the equivalent output voltage can be written as

$$e_0(t) = e_B \left[\frac{K_1 \, \epsilon(t)}{4 + 2K_1 \, \epsilon(t)} \right]$$

or for low gage factors and small strains this can be simplified to

$$e_0(t) \approx e_B \left[\frac{K_1 \, \epsilon(t)}{4} \right]$$

The output impedance of the bridge will be a function of time since it is the resistance of the gage that is varying. However, the magnitude of this variation should be small and since the bridge output will be connected to a high impedance, it will be assumed that $R_g(t)$ has a constant value of 120 ohms. Then Z_0 in Figure 31 is purely resistive and can be seen to be 120 ohms.

Examination of Figures 29 and 30 shows that the series resistance and inductance in the transducer to amplifier cable $\left[\left(A'\right) \text{ to } \left(F\right)\right]$ attenuate the voltage into the amplifier input. This attenuation can be described as follows

$$\text{attenuation} = \frac{Z_P}{Z_S + Z_P} \quad \text{where} \quad f = 10 \text{ kc}$$

$$Z_S = R_4 + j X_L = 5 + j \, 1.3$$

$$Z_P = (R_i)(-j X_{C_i}) \Big/ \left(R_i - j X_{C_i} \right) = 9.1 \times 10^4 - j \, 2.9 \times 10^4$$

81

Hence Z_S can be neglected. It can also be shown that R_5 and X_C in series with C_1 can be neglected. The equivalent circuit of the Wheatstone bridge simplifies further to that shown in Figure 32.
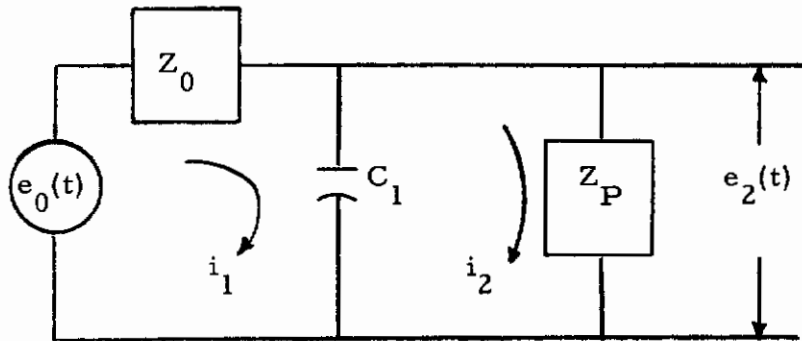
Figure 32. Further Simplification of the Wheatstone Bridge and Cable Circuitry

$$e_2(t) = e_0(t) \left[\frac{Z_P}{Z_0 + Z_P + Z_0 \dfrac{Z_P}{X_{C_1}}} \right]$$

$$= e_0(t) \left[\frac{9.1 \times 10^4 - j\,2.9 \times 10^4}{120 + 9.1 \times 10^4 - j\,2.9 \times 10^4 + (120) \dfrac{9.1 \times 10^4 - j\,2.9 \times 10^4}{-j\,3.2 \times 10^3}} \right]$$

$$e_2(t) \approx e_0(t) \; \underline{/0^\circ}$$

Thus, the shunt capacitance of the transducer to amplifier cable and the input capacitance of the amplifier can be neglected.

In summary, the frequency response function between the voltage across the strain gage and the voltage developed at the input to the amplifier section of the signal conditioner is independent of frequency if the assumed values for impedance are as large or larger than those actually occurring at the Sonic Fatigue Facility.

82

4.3.3 Signal Conditioner

The signal conditioners used for the measurement of strain at the Sonic Fatigue Facility are quite similar to those used for the measurement of vibration and acoustic levels. The only differences are

(1) The impedance converter is not used for strain measurement.

(2) DC bridge excitation voltage is added.

(3) Bridge circuitry is added.

Since the remaining portions of the signal conditioner, two stages of amplification and a differential isolator, have been discussed in the accelerometer section, only the differences occurring in the strain measuring circuitry will be considered here.

Similar to the development in Section 2.4.3, the voltage due to internal noise occurring on the output of the signal conditioner when both amplifiers are set at a gain of 100 is

$$e_N = (100) \sqrt{\left[(100)(A)(w)\right]^2 + y^2} \qquad (68)$$

$$w = \sqrt{e_d^2 + e_b^2 + \left(\frac{e_c}{100}\right)^2} \qquad (69)$$

where

e_N = the output noise voltage of the signal conditioner in volts rms

y = the equivalent input noise voltage of the second amplifier in volts rms

A = the total "gain" in the normalizing and automatic attenuators

e_d = the noise voltage out of the bridge due to power supply noise in volts rms

e_b = the equivalent input noise voltage of the first amplifier in volts rms

e_c = the equivalent input noise voltage of the differential isolator in volts rms

83

The value of the noise voltage out of the bridge due to power supply noise will be equal to or less than the product of strain, gage factor, and power supply noise voltage (e_{BN}). If the values of the bridge resistors are assumed to be equal to each other and to the zero strain value of the strain gage, the output of the bridge due to power supply noise is found by replacing the DC excitation voltage in Eq. (55) with the power supply noise voltage. Thus,

$$e_d(t) = \left[e_{BN}(t) \right] \left(\frac{K_1 \, \epsilon(t)}{4 + 2 K_1 \epsilon(t)} \right) \tag{70}$$

or

$$e_d \leq (e_{BN}) \left(\frac{K \epsilon}{4} \right) \tag{71}$$

where

    $e_d(t)$ = the instantaneous noise voltage out of the bridge due to power supply noise

    $e_{BN}(t)$ = the instantaneous noise voltage of the power supply

    e_{BN} = the rms noise voltage of the power supply

    ϵ = the rms strain

It is extremely important to minimize the ratio of the power supply noise voltage to the quiescent power supply voltage. To illustrate this, a signal-to-noise ratio (S/N) will be defined as the ratio of the rms value of the output of the bridge due to applied strain to the rms value of the output of this same bridge to power supply noise.

$$(S/N)_1 = \frac{e_2}{e_d} = \frac{e_B \left(\frac{K_1 \epsilon}{4} \right)}{e_{BN} \left(\frac{K_1 \epsilon}{4} \right)} = \frac{e_B}{e_{BN}} \tag{72}$$

84

Thus it can be seen that the signal-to-noise ratio at the output of the bridge is equal to the DC value of the bridge excitation voltage divided by the rms value of the power supply noise. Since the signal-to-noise ratio can only decrease from its value at the output of the bridge, it can be seen that it is quite important to maximize this ratio.

Similar to Eq. (25) of Section 2.4.3, the total DC drift voltage on the output of the signal conditioner, when both amplifiers have gains of 100 and the Wheatstone bridge is balanced, is

$$e_D = (100) \left\{ \left[(e_{bD})(100) + e_{cD} \right] (A) + y_D \right\} \qquad (73)$$

where

e_D = the output of the signal conditioner, due to drift, in volts DC

e_{bD} = the equivalent input voltage to the first amplifier, due to drift, in volts DC

e_{cD} = the equivalent input voltage to the differential isolator, due to drift, in volts DC

A = the total "gain" in the normalizing and automatic attenuators

y_D = the equivalent input voltage to the second amplifier, due to drift, in volts DC

If the bridge is not balanced, the value of e_D is

$$e_D = (100) \left\{ \left[(e_{BD} + e_{bD})(100) + e_{cD} \right] (A) + y_D \right\} \quad (74)$$

where

e_{BD} = the DC voltage out of the Wheatstone bridge, for zero applied strain, due to unbalance of the bridge

Notice that any change in the value of the DC excitation voltage can have two effects. First, if the bridge is unbalanced, the DC unbalance

85

voltage on both the output of the bridge and the output of the signal conditioner will change.

$$\Delta e_{BD} = \left(e_{B_1} - e_{B_2}\right)\left(\frac{R_B}{R_B + R_C} - \frac{R_A}{R_A + R_{g_1}}\right) \qquad (75)$$

where

Δe_{BD} = the change in unbalance voltage on the output of the bridge

e_{B_1}, e_{B_2} = the DC bridge excitation voltage at times, t_1 and t_2, respectively

R_A, R_B, R_C, R_{g_1} = bridge resistors as defined in Figure 23

Secondly, and generally more importantly, the sensitivity (volts out of the signal conditioner for a given strain) of the entire strain measuring system will vary. To more clearly illustrate this error source, the bridge resistors will be assumed to be equal to each other and the zero strain value of the strain gage resistance. Also, the value of all of the DC drift voltages, except that in the power supply, will be assumed to be zero. In this case

$$e_3(t) = K_3 e_2(t) = (K_3)(e_B)\left(\frac{K_1 \epsilon(t)}{4 + 2K_1 \epsilon(t)}\right)$$

The percent error in the output of the signal conditioner due to a drift in the value of DC bridge excitation voltage is

$$\% \text{ error} = 100\left(\frac{e_{B_2}}{e_{B_1}} - 1\right) \qquad (76)$$

Or, stated another way, an x% change in DC bridge excitation voltage results in a corresponding x% change in the measurement error. It is quite important

86

that the bridge excitation voltage be highly stable if strain amplitudes are to be measured accurately.

One of the inherent inaccuracies of a Wheatstone bridge for the measurement of dynamic resistance changes, or for that matter, any unbalanced operation is that the output of the bridge is a nonlinear function of the resistance being measured. The wheatstone bridge was originally conceived for the null-balance measurement of unknown resistance values. These resistance values were fixed so there was essentially no problem in balancing the bridge and avoiding the nonlinearities inherent in unbalanced operation. It was entirely natural that this circuit would be used with strain gages to measure static strain, and then later, because the change in resistance of the strain was a very small percentage of the total resistance of the strain gage, it was natural to neglect the small error due to this nonlinearity and use the Wheatstone bridge circuit for the measurement of periodic strains. However, when used for the measurement of strains whose amplitude varies randomly with time, the Wheatstone bridge circuit can introduce very large errors. Since unbounded random processes have a finite probability of exceeding any given amplitude level, and since the voltage out of the Wheatstone bridge limits at a finite amplitude, one could theoretically have an infinite error in the measurement of resistance, or strain. While in the practical case one is not too concerned with measuring infinite strains, one must be concerned about the distortion of the amplitude probability density function at high strain levels caused by the use of a Wheatstone bridge circuit. For a normally distributed applied strain, the output of the Wheatstone bridge will approach a truncated normal distribution because the Wheatstone bridge nonlinearity is of the saturation type. From Eq. (56), the percent error in the measured strain amplitude is

$$\% \text{ error} = \left[\frac{K_1 \epsilon(t)}{2}\right] (100)$$

87

For wire and foil strain gages, K_1 is approximately equal to 2, so the percent error in the indicated strain amplitude is approximately equal to the percent strain. For semiconductor strain gages, K_1 can be equal to 100 or 200. Therefore, the percent error can be from 50 to 100 times the percent strain.

4.3.4 Other Considerations

The preceding sections have in general assumed balanced bridge operation, equal bridge resistors, and only one active bridge arm. These assumptions were made to more clearly describe the particular error source being discussed, but are not necessary to the operation of the strain gage systems. Therefore, the results of not making these assumptions will be discussed in this section.

The effects of unbalance on a Wheatstone bridge can be studied by writing the equation for the output voltage of the circuit in Figure 24.

$$e_2(t) = e_B \left(\frac{1}{2} - \frac{R}{R + R_g(t)} \right)$$

Let $R_g(t) = (R + R_1)\left[1 + K\epsilon(t) \right]$ where the zero strain value of $R_g(t)$ is greater than R by R_1 ohms. Now,

$$e_2(t) = e_B \left\{ \left[\frac{R_1}{2(2R + R_1)\ 1 + K\epsilon(t)} \right] + \left[\frac{K_1 \epsilon(t)}{2\left(\frac{2R + R_1}{R + R_1} \right)\left[1 + K\epsilon(t) \right]} \right] \right\} \quad (77)$$

If it can be correctly assumed that $R_1 \ll R$, and $K\epsilon(t) \ll 1$, then this can be simplified to

$$e_2(t) \approx e_B \left\{ \frac{R_1}{4R} + \frac{K_1 \epsilon(t)}{4} \right\} \quad (78)$$

This is simply the sum of the unbalance voltage, and the voltage due to the strain. It is good practice to operate with a balanced bridge circuit even if

88

the above assumptions can be correctly made in order to prevent "one-sided" saturation by either the tape recorder or the signal conditioner amplifiers. (These devices are designed for a maximum dynamic range with a zero mean input.)

The use of equal value bridge resistors greatly simplifies the calculations required to demonstrate the operation of a Wheatstone bridge, but it is not necessary, and in fact, in some cases it is undesirable to use equal resistances. Figure 33 shows the circuit diagram of two other bridge arrangements.
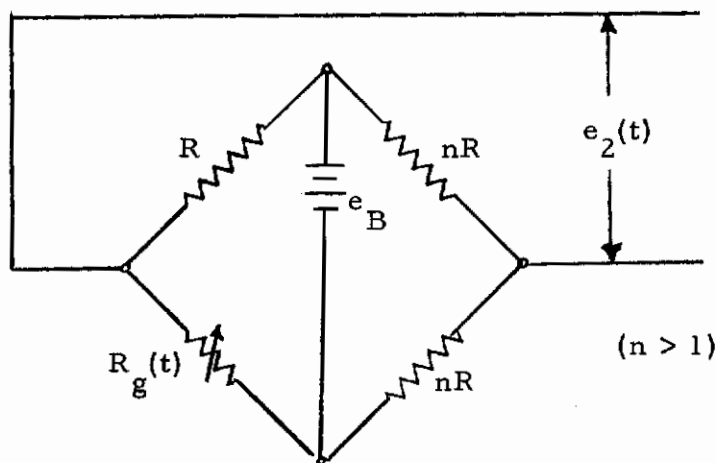
(a) Excitation Source Connected to Junctions of Unequal Resistors
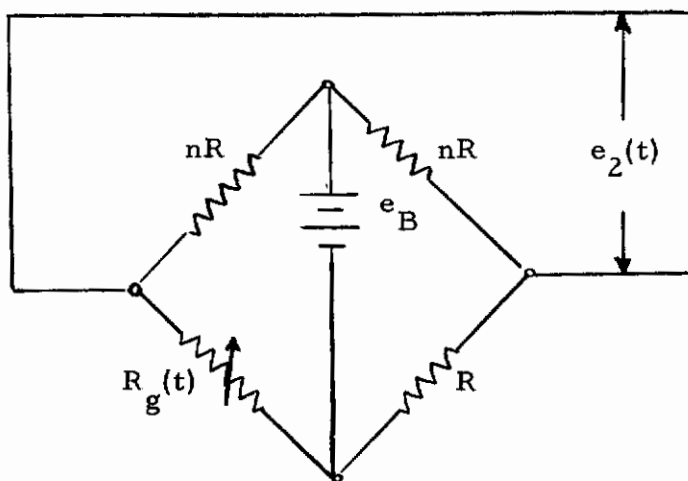
(b) Excitation Source Connected to Junctions of Equal Resistors

Figure 33. Circuit Diagrams of Wheatstone Bridges

To study the performance of these bridges, the total excitation current required, and the output voltage for a given strain of each bridge will be compared to the performance of an "equal-arm" bridge. The total excitation current required by the "equal-arm" bridge of Figure 24 under balance conditions is

$$I_T = (e_B)\left(\frac{1}{R}\right) \tag{79}$$

where

I_T = the total excitation current at balance in amperes DC

$R_g(t) = R\left[1 + K\epsilon(t)\right] = R$ at $t = 0$ or at balance

The output voltage for a given excitation voltage is given in Eq. (55) as

$$e_2(t) = \frac{(e_B)\left[K_1\epsilon(t)\right]}{4 + 2K_1\epsilon(t)}$$

The comparable equations for the circuit in Figure 33a are

$$I_T = (e_B)\left[\frac{n+1}{2nR}\right] \tag{80}$$

$$e_2(t) = \frac{(e_B)\left[K_1\epsilon(t)\right]}{4 + 2K_1\epsilon(t)} \tag{81}$$

and the comparable equations for the circuit in Figure 33b are

$$I_T = (e_B)\left[\frac{2}{(n+1)R}\right] \tag{82}$$

$$e_2(t) = (e_B)\left(\frac{n}{(n+1)}\right)\left[\frac{K\epsilon(t)}{(n+1) + K\epsilon(t)}\right] \tag{83}$$

From the above equations, it can be seen that the circuit in Figure 33a requires less current than the "equal-arm" bridge while still maintaining

90

the same output sensitivity. It can also be seen that the circuit in Figure 33b requires the least current, but also has the least output sensitivity.

The cable arrangement at the Sonic Fatigue Facility permits the use of either one or two strain gages per channel. If two strain gages are used, the particular cabling arrangement constrains the gages to adjacent bridge arms. This somewhat restricts the usefulness of this feature. However, two gages in adjacent bridge arms can be used quite effectively for the measurement of bending stresses by placing one of the gages on the upper surface of the test specimen and one of the gages on lower surface of the test specimen as shown in Figure 34.
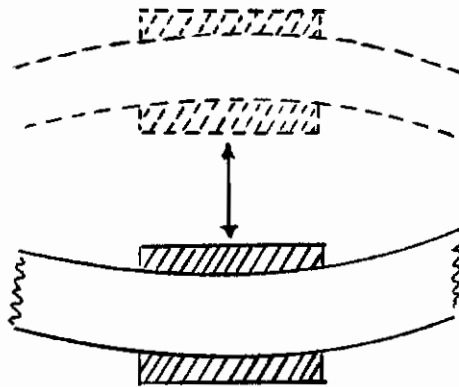

Figure 34. Two Strain Gage Method of
Measuring Bending Strains

As the test specimen bends, one gage increases in resistance and the other decreases in resistance. This has two benefits that can be seen from the equation for the output of the Wheatstone bridge circuit shown in Figure 35.

91
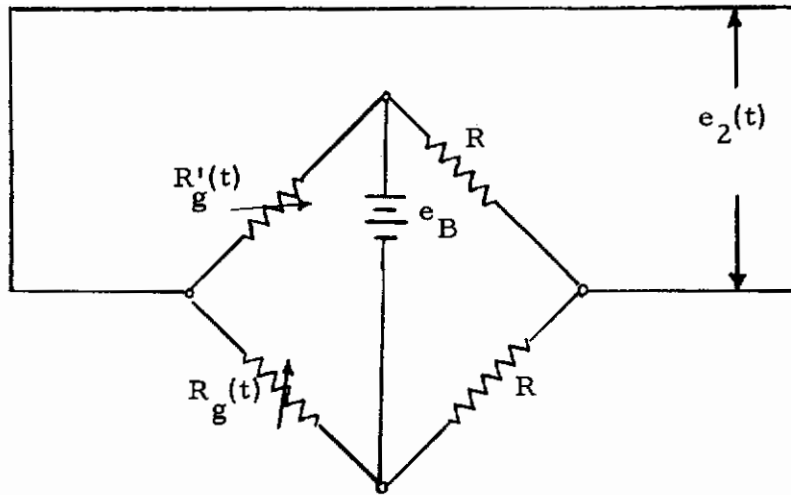
Figure 35. Wheatstone Bridge Circuit
for Two Strain Gages in
Adjacent Arms

$$e_2(t) = e_B \left(\frac{R}{2R} - \frac{R'_g(t)}{R'_g(t) + R_g(t)} \right)$$

$$R_g(t) = R \left[1 + K_1 \epsilon(t) \right]$$

$$R'_g(t) = R \left[1 - K_1 \epsilon(t) \right]$$

$$e_2(t) = e_B \left(\frac{K_1 \epsilon(t)}{2} \right) \tag{84}$$

Comparison of Eqs. (84) and (55) reveal that the use of two gages in the manner described makes the output of the Wheatstone bridge linear, and doubles the output sensitivity of the bridge. Outputs due to both temperature variations and longitudinal strains are cancelled with this arrangement.

The two gage arrangement can be used to measure longitudinal strains with the same result as shown in Eq. (84) only when the two strain gages have gage factors of opposite polarity because the gages are in adjacent bridge arms.

Two gages are also sometimes used to measure longitudinal strains by orienting one gage, $R_g(t)$, with its sensitive axis in the longitudinal direction and the second gage, $R'_g(t)$, perpendicular to the first gage as shown in Figure 36. This arrangement is used to cancel the effects of temperature variations.
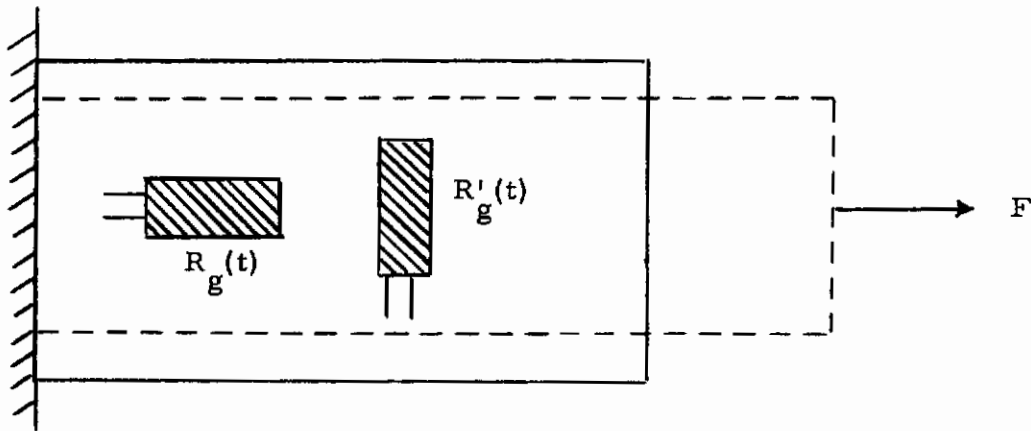
Figure 36. Two Gage Adjacent Arm Measurement of Longitudinal Strain

The value of $R'_g(t)$ is

$$R'_g(t) = R\left[1 + \mu K_1 \epsilon(t)\right]$$

where

μ = Poisson's ratio of the test specimen

The output of the Wheatstone bridge circuit shown in Figure 35 is

$$e_2(t) = (e_B)\left\{\frac{(1 + \mu)K_1 \epsilon(t)}{2\left[2 + (1 - \mu)K_1 \epsilon(t)\right]}\right\} \tag{85}$$

Comparison of this equation to Eq. (55) shows that the output sensitivity has been increased by approximately $(1 + \mu)$.

93

4.4 ENVIRONMENTAL INACCURACIES

Both temperature and relative humidity variations can cause inaccuracies in the measurement of resistance with bonded variable resistance strain gages. These are the primary environmental inaccuracies that will be encountered during strain measurement in the Sonic Fatigue Facility.

Relative humidity can cause inaccuracies in two manners. Reference [41] states "One of the principal causes of gage instability is moisture which is absorbed into the body of the gage. The effects of moisture are (a) dimensional changes of the bonding medium and cement which causes resistance changes due to the resulting strains set up in the gage filament, and (b) changes of resistances due to the conductivity and corrosion of the strain sensing materials caused by absorbed moisture."

There are three basic manners in which the inaccuracy to relative humidity can be reduced. In order of preference, these are

(1) Control the relative humidity to which the strain gages are exposed.

(2) Use the strain gages and the cements that are the least susceptible to the humidity.

(3) Moisture-proof the strain gage installation.

The sensitivity of strain gages to temperature variations will probably be the greatest source of environment related inaccuracies encountered at the Sonic Fatigue Facility. Temperature changes can effect both the resistance of the strain gage and the strain gage leads.

If the temperature of the test specimen and strain gage is increased, the test specimen will elongate. This will cause the resistance of the strain gage to change and indicate this strain. The cement and gage material will also elongate and cause additional strain to be indicated. And, in addition,

94

the resistance of the variable resistance material of the strain gage will change due to the temperature change. The resulting "apparent strain" can be written as follows

$$\epsilon_a = \beta_1 + \beta_2 + \frac{\alpha}{K_1} \tag{86}$$

where

ϵ_a = the apparent strain due to a temperature change (dimensionless or inches/inch)

β_1 = the thermal coefficient of expansion of the test specimen (in inches/inch per ^oF)

β_2 = the thermal coefficient of expansion of the strain gage/cement combination (in inches/inch per ^oF)

α = the temperature coefficient of resistance (in ohms/ohm per ^oF)

K_1 = the gage factor of the strain gage

For most practical applications it would be desirable to have the "apparent strain" equal to zero for all temperatures of interest. There are two methods by which this ideal situation is approached in the construction of the strain gage. First, a variable resistance element that has a negative thermal coefficient of resistance can be selected. (Constantan is such a material.) The value of thermal coefficient is selected so that

$$\alpha = K_1 (\beta_1 + \beta_2)$$

Unfortunately, none of the above thermal coefficients are linear functions of temperature so that this technique only works over a limited temperature range. An "apparent strain" tolerance of $\pm 1 \mu$ in/in per ^oF over a range of temperatures from -50 to +350^oF is quoted in Ref. [42].

The second method is to select a gage with a negative gage factor such that

$$K_1 = \frac{\alpha}{\beta_1 + \beta_2}$$

95

The preceding comments on nonlinearity of thermal coefficients applies to these gages also. An apparent strain of 6μ in/in per ^{o}F is quoted as typical for the type of gage in Ref. $[43]$. Both of the above techniques require that the gage be designed for the particular material that is used in the test specimen.

Several other techniques have been used in the construction of strain gages to minimize their temperature sensitivity (Ref. $[43]$). Gages have been constructed with a combination of positive and negative temperature coefficients of resistance to reduce the nonlinearity effects. These gages are advertised as having a $\pm 1/4\mu$ in/in per ^{o}F tolerance on apparent strain over their rated temperature range. Another technique that has been used primarily for the construction of high temperature strain gages is to include a portion of the adjacent bridge arm resistance in the gage. This portion of the adjacent arm resistance is a temperature sensitive element. By adjusting the remaining resistance of this adjacent arm, one can vary the apparent strain. Apparent strain tolerances of $\pm 1/10\mu$ in/in per ^{o}F are advertised as the temperature sensitivity tolerances for this type of strain gage.

If it is not desired to use a strain gage with some built-in temperature compensation, then multiple gages can be used as discussed in Section 4.3.4. Or, one can use a temperature sensitive, strain insensitive resistance element for the adjacent arm of the bridge and expose it to the same temperature. Frequently a strain gage of the same type as is used for the strain measurement is used as the temperature compensation by mounting it on to material with identical thermal characteristics to that of the test specimen. This technique will not be of much value in the Sonic Fatigue Facility since it would be extremely difficult to isolate the gage being used for temperature compensation from strains.

One other temperature related inaccuracy that may occur on rare occasions is due to the Seebeck effect. If there is an appreciable thermal

96

gradient between the junctions of the strain gage leads, an electromotive force will be developed due to the contact of the dissimilar materials used in the strain gage and the wires to the signal conditioner.

Compensation for thermally induced changes in the resistance of the wires from the strain gage(s) to the signal conditioner can be accomplished as described in Section 4.3.2 by using three wires for either one or two gage operation. Both of the wires to the bridge will be of equal length and will be routed together so that they will be exposed to the same temperature making both wires of almost identical resistance. The wire to the signal conditioner does not need to be equal to the wires between the bridge and gage length or resistance. If the wires are attached as shown in Figure 37a and 37b, the change in resistance of the lead wires will not unbalance the bridge. These wiring arrangements place the bridge lead resistances (R_L) in adjacent bridge arms and since their values are equal they will cancel. The variation of R_{L_2} is unimportant (assuming of course that a high input impedance amplifier is being used). One effect in variation of the lead wire resistance that cannot be balanced out is the change in apparent gage factor as the ratio of R_g/R_L changes.
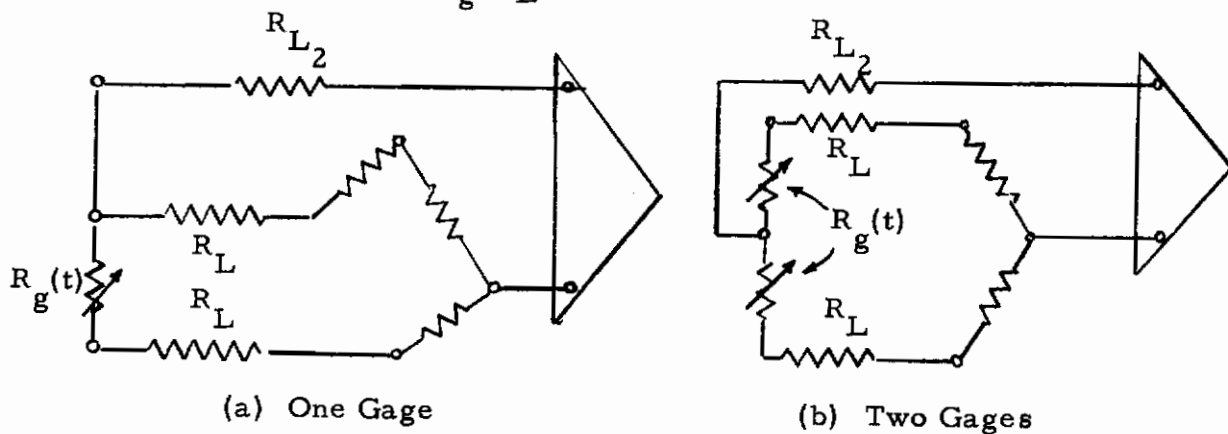

(a) One Gage   (b) Two Gages

Figure 37. Three Wire Connections for One and Two Strain Gages

97

4.5   USAGE INACCURACIES

Strain gage usage inaccuracies occur in the following phases:

(1)   Selecting the proper location to make measurements.

(2)   Installing the strain gage properly.

(3)   Calibrating the strain gage system properly.

(4)   Properly performing the measurements.

Since a good deal of the usage errors have been previously covered in Sections 2 and 3 of this report, only the usage inaccuracies peculiar to strain gages will be discussed in the following paragraphs.

The "proper" location for installation of a strain gage for any particular measurement may be the result of response calculations, experimental response measurements, engineering judgment, or the need to duplicate a location used in some previous test. Obviously, guidelines can only be given for performing experimental response measurements.

A convenient method of experimentally determining the location of the points of maximum stress is by the use of a brittle lacquer coating. The test specimen is coated with this lacquer and then subjected to a test environment. The lacquer will develop cracks at points of high stress concentration. From these cracks one can also determine the strain orientation and concentration pattern, and to a limited extent, the strain magnitude. For more information on this technique, see Ref. [44].

Mounting of the strain gage will probably be the largest source of usage inaccuracies encountered. In particular, soldering of the strain gage leads to the cabling, and bonding of the strain gage to the test specimen are the two most important aspects to be considered in mounting a strain gage. A poor soldering job will result in an increase in the resistance of the solder joint with time, and perhaps catastrophic failure of the joint. Poor bonding will result in the strain gage not faithfully transducing the strain of the test specimen, and in severe cases, catastrophic failure of the

98

gage. It is not the purpose of this report to provide an instruction manual for the installation of strain gages. For this information, see Refs. [41, 45, 46].

Other mounting problems include orientation of the strain gage along the axis of greatest strain, minimizing static loading, and minimizing strain gradient effects. The brittle-lacquer method of determining mounting locations also shows the strain orientation. However, if it is not desired to use this method, the orientation and amplitude of the maximum strain can be found by the use of rosette type strain gages.

For dynamic strain measurements of a test specimen under a large static strain, the strain gage should be installed after the test specimen has been attached to the test fixture in order to minimize the static strain of the gage. Large static strains can cause inaccuracies in the measurement of dynamic strain by causing "creep" of the strain gage. (For discussions of the creep characteristics of various types of strain gages and cements, see Refs. [33, 34, 36, 47].)

Since the output of a strain gage is an average of the strains developed over the surface of the gage, it is difficult to make accurate strain measurements over an area that has a high strain gradient. To minimize this type of inaccuracy, the smallest size suitable strain gage should be selected for measurements in areas where strain gradients exist. (The smaller the size of the strain gage - the less surface averaging that takes place.)

The calibration of strain gage systems for the measurement of dynamic strains leaves a lot to be desired. Static calibrations can be made with a very high degree of accuracy and, for a few specialized cases, dynamic strain calibration can be performed with reasonable accuracy by the measurement of some other parameter, such as displacement. However, for most cases, dynamic strain calibration is impossible.

This is simply because:

(1)   there is no device presently available that will supply an accurately known strain at any frequency between 0 and 100 kc to all possible configurations of test specimens, and

(2)   the strain gage cannot be attached to a separate calibration device, as can an accelerometer or microphone, because the strain gage would be destroyed in attempting to break the gage/ calibration surface bond.

Therefore, a total system dynamic calibration is generally not feasible. One must either accept the gage factor stated by the manufacturer or perform a static strain calibration to obtain the DC sensitivity of the strain gage. Then the frequency response function of the gage must be determined analytically. The remainder of the strain measuring system can be readily calibrated by either dynamic or static means.

The signal conditioners at the Sonic Fatigue Facility have built in resistors for performing a DC electrical calibration of the strain measuring system. The circuit arrangement is as shown in Figure 38. Since the calibration resistor is applied across the adjacent arm, the bridge output voltage will be opposite in polarity to that due to shunting the transducer arm. The value of the calibration resistor (R_C) for a given static strain (ϵ) is

$$R_C = \left(\frac{R + 2R_L + \frac{|R_L|^2}{R}}{K_1 |\epsilon|} \right) - R - R_L \quad \text{assuming } R_{L_2} \ll R_C \text{ and} \tag{87}$$

$$R_g(t) = R + RK\epsilon(t)$$

100
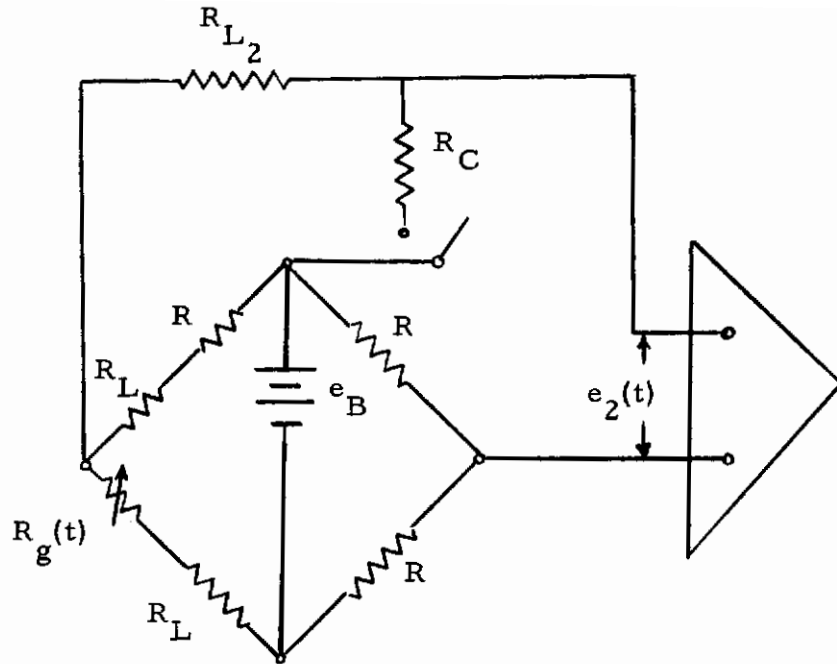
Figure 38. Three Wire Shunt Calibration of a Wheatstone Bridge

Because in practice $R_L \ll R$, Eq. (87) can be generally simplified to the following form.

$$R_C = \left(\frac{R + 2R_L}{K_1 |\epsilon|} \right) - R \qquad (88)$$

Note that the lead resistance values must be included in the calculation of R_C for this to be an accurate calibration. $\left(R_C \neq \frac{R}{K|\epsilon|} \right)$. The value of calibration resistor required to simulate a given static strain when two identical strain gages are used in the bridge circuit of Figure 38 is

$$R_C = \left(\frac{R + R_L}{2K_1 |\epsilon|} \right) - \frac{R}{2} - \frac{R_L}{2} \qquad (89)$$

101

which can be simplified to

$$R_C = \left(\frac{R + R_L}{2K_1 |\epsilon|} \right) - \frac{R}{2} \qquad (90)$$

One final usage inaccuracy that must be kept in mind is due to self-heating of the strain gages. The heat in calories generated by a strain gage will be approximately

$$\frac{(.06)(e_B^2)}{R} t$$

where R is the resistance in ohms at all the bridge arms at balance, and t is time in seconds. The zero strain resistance of the strain gage will be

$$R_{g_2} \approx R_{g_1} \left[1 + \alpha(T_2 - T_1) \right] \qquad (91)$$

where

R_{g_2} = the zero strain resistance of the strain gage at temperature T_2

R_{g_1} = the zero strain resistance of the strain gage at temperature T_1

α = the temperature coefficient of resistance

T_1 = the temperature of the strain gage before voltage is applied to the bridge circuit

T_2 = the equilibrium temperature of the strain gage after voltage has been applied to the bridge circuit.

The two important points are:
  (1) Select a value of excitation voltage such that the strain gage will reach a reasonable equilibrium temperature.
  (2) Balance the bridge, and perform measurements, after the strain gage has reached its equilibrium temperature.

102

REFERENCES

1. Korn, G.A., and T.M.Korn, Electronic Analog Computers, McGraw-Hill Book Co., Inc., New York. 1952.

2. Sheingold, D.H., "Impedance and Admittance Transformations Using Operational Amplifiers," The Lighting Empiricist, vol. 12, No. 1, pp. 1, 2, 7, and 8. January 1964.

3. Waltrip, D., "Operational Amplifiers: Their Specification and Use," Data Systems Engineering, pp. 34-47. July-August 1963.

4. Eshbach, O.N., Handbook of Engineering Fundamentals, John Wiley and Sons, Inc., New York. 1954.

5. Minnar, E.J., ISA Transducer Compendium, Plenum Press, New York. 1963.

6. Harris, C.M. and C.E. Crede, Shock and Vibration Handbook, vol. 1, Chapter 16, p. 19, McGraw-Hill Book Co., Inc. New York. 1961.

7. Tengwall, R., "Selection of Accelerometer for Flat Frequency Response," Endevco Tech-Data No. 583. April 1963.

8. White, G., "Response Characteristics of a Simple Instrument," Statham Laboratories Instrument Notes No. 2. April-May 1948.

9. Harris, C.M. and C.E. Crede, Shock and Vibration Handbook, vol. 1, Chapter 12, p. 5, McGraw-Hill Book Co., Inc. New York. 1961.

10. Bouche, R.R., "High Frequency Response and Transient Motion Performance Characteristics of Piezoelectric Accelerometers," ISA Fall Instrument Automation Conference and Exhibit, Los Angeles, California. September 1961.

11. Daniel, Mann, Johnson and Mendenhall Drawing No. IN6, "Vibration Channel," prepared for WADC, WPAFB, Ohio.

12. Piersol, A.G., "The Measurement and Interpretation of Ordinary Power Spectra for Vibration Problems," prepared by MAC under Contract NAS-5-4590, and being issued by Goddard Space Flight Center as a NASA Contractor Report.

13. Rhodes, J.E., "Evaluation of Crystal Transducers Throughout Wide Temperature Ranges," Endevco Tech-Data No. 556. March 1963.

14. Harris, C.M. and C.E. Crede, Shock and Vibration Handbook, vol. 1, Chapter 6, pp. 22-23 and 31-34. McGraw-Hill Book Co., Inc. New York. 1961.

15. Epstein, B., "Acoustic Sensitivity of Accelerometers," Endevco Tech-Data No. 577. January 1963.

16. Endevco Corporation Accelerometer Sales Catalog

17. Gulton Industries Accelerometer Sales Catalog

18. Columbia Research Laboratories Accelerometer Sales Catalog

19. Bradley, W., Jr., "Effects of High Intensity Acoustic Fields on Crystal Vibration Pickups," 26th Shock and Vibration Symposium, Washington, D.C. December 1958.

20. Gulton Industries Sales Bulletin A10, "Glennite Self Generating Accelerometer," Model A-3100T.

21. Harris, C.M. and C.E. Crede, Shock and Vibration Handbook, vol. 1, Chapter 19, p. 10, McGraw-Hill Book Co., Inc. New York. 1961.

22. Beranek, L.L., Noise Reduction, p. 111, McGraw-Hill Book Co., Inc. New York. 1960.

23. Crandall, S.H. et al, Random Vibration, Technology Press, Massachusetts Institute of Technology. 1958.

24. B&K Instruments, Inc. Catalog Sheet C1-NM 135, 1960.

25. Kistler Instrument Corporation Sales Catalog

26. Brüel and Kjaer Instruction and Application Manual, "Condenser Microphones Type 4131/4132," October 1960.

27. Beranek, L.L. Noise Reduction, p. 126-127, McGraw-Hill Book Co., Inc. New York. 1960.

28. Brüel and Kjaer Instruction and Application Manual, "Microphone Calibration Apparatus Type 4142," February 1962.

29. Brüel, P.V. and G. Rasmussen, "Free Field Response of Condenser Microphones," Technical Review, No. 1, pp. 12-17. January 1959.

30. ———————————————— "Free Field Response of Condenser Microphones (Part II)," Technical Review, No. 2, pp. 1-15. April 1959.

31. Harris, C.M. and C.E. Crede, Shock and Vibration Handbook, vol. 1, Chapter 17, p. 19, McGraw-Hill Book Co., Inc., New York. 1961.

32. Baldwin-Lima-Hamilton Technical Data No. 4310-3, "SR-4 Strain Gage Evaluation Report," March 1958.

33. ——————————————— Technical Data No. 4310-6, "SR-4 Strain Gage Performance Summary," October 1958.

34. ——————————————— Technical Data No. 4310-7, "SR-4 Strain Gage Evaluation (Continued)," May 1959.

35. Baldwin-Lima-Hamilton Technical Data No. 4310-2, "SR-4 Strain Gage Bonding Cement Evaluation Report," March 1958.

36. ——————————————— Technical Data No. 4310-8, "SR-4 Strain Gage Bonding Cement Evaluation (Continued)," May 1959.

37. ——————————————— Technical Data No. 4310-5, "SR-4 Strain Gage Performance Report Gage Factors at High Strains," October 1958 (revised May 1963).

38. Wolf, N.D., "Summary of Strain Gage Fatigue Data," ASD-TDR-63-202, Aeronautical Systems Division, AFSC, USAF, WPAFB, Ohio. April 1963.

39. Smith, P.W., Jr., Starr, E.A., Dietrich, C.W., and D.U. Noiseux, "Study of a Response Load Recorder," vol. II, ASD-TDR-62-165, Aeronautical Systems Division, AFSC, USAF, WPAFB, Ohio. March 1963.

40. Harris, C.M. and C.E. Crede, Shock and Vibration Handbook, vol. 1, Chapter 17, p. 9, McGraw-Hill Book Co., Inc., New York 1961.

41. Baldwin-Lima-Hamilton Corp., "Strain Gage Handbook."

42. ——————————————— Strain Gage Sales Catalog No. 4310-62.

43. Kulite-Bytrex Corporation, Semiconductor Strain Gage Sales Bulletin K-101.

44. Perry, C.C. and H.R. Lissner, The Strain Gage Primer, Chapter 13, McGraw-Hill Book Co., Inc., New York. 2d Ed. 1962.

45. Harris, C.M. and C.E. Crede, Shock and Vibration Handbook, vol. 1, Chapter 17, pp. 32-42, McGraw-Hill Book Co., Inc. New York. 1961.

46. Perry C.C. and H.R. Lissner, The Strain Gage Primer, Chapter 3, McGraw-Hill Book Co., Inc., New York. 2d Ed. 1962.

47. Baldwin-Lima-Hamilton Technical Data No. 4310-4, "SR-4 Strain Gage Performance Report," October 1958.

SUMMARY OF IMPORTANT EQUATIONS

1. The voltage developed at the input to a voltage amplifier by a piezo-electric accelerometer or microphone in terms of the charge sensitivity of the transducer is

$$e_2 = \frac{\ddot{x} S_1}{C_a + C_c + C_i}$$

Eq. (3)
page 8

2. The frequency response function of a typical accelerometer is

$$H_1(f) = (C_1) \left[\frac{1}{(2\pi f_n)^2} \right] \left[\frac{1}{\sqrt{\left[1 - \left(\frac{f}{f_n} \right)^2 \right]^2 + \left[2\zeta \frac{f}{f_n} \right]^2}} \right] \left[e^{j\phi(f)} \right]$$

Eq. (19)
page 18

$$\phi(f) = \tan^{-1} \left[\frac{2\zeta \frac{f}{f_n}}{1 - \left(\frac{f}{f_n} \right)^2} \right]$$

Eq. (21)
page 18

3. The ratio of the voltage developed at the input to a voltage amplifier to the open circuit voltage of a piezoelectric accelerometer or microphone is

$$\frac{e_2}{e_1} = \left(\frac{C_a}{C_a + C_c + C_i} \right) \left[\frac{1}{1 + \frac{1}{2\pi j f (R_i)(C_a + C_c + C_i)}} \right]$$

Eq. (26)
page 29

4. The frequency response function (pressure response) of a typical microphone is

$$H_1(f) = \frac{K_1 e^{j\phi_1(f)}}{\sqrt{\left[1 - \left(\frac{f}{f_n} \right)^2 \right]^2 + \left[2\zeta \frac{f}{f_n} \right]^2}}$$

Eq. (28)
page 44

106

$$\phi_1(f) = -\tan^{-1}\left[\frac{2\zeta\dfrac{f}{f_n}}{1 - \left(\dfrac{f}{f_n}\right)^2}\right]$$

Eq. (29)
page 44

5. The voltage out of a Wheatstone bridge, when all of the bridge arms have equal resistance at zero strain, is

    (a) For one active bridge arm

$$e_2(t) = \frac{e_B\left[K_1\,\epsilon(t)\right]}{4 + 2K_1\,\epsilon(t)}$$

Eq. (55)
page 66

    (b) For two active adjacent bridge arms arranged so that the resistance changes in the two gages are equal and opposite for any given strain

$$e_2(t) = \frac{e_B\left[K_1\,\epsilon(t)\right]}{2}$$

Eq. (84)
page 92

6. The value of calibration resistance required for three wire shunt calibration of a Wheatstone bridge is

$$R_C = \left(\frac{R + 2R_L}{K_1|\epsilon|}\right) - R$$

Eq. (88)
page 101

DOCUMENT CONTROL DATA - R&D		
(Security classification of title, body of abstract and indexing annotation must be entered when the overall report is classified)		

1. ORIGINATING ACTIVITY *(Corporate author)*	2a. REPORT SECURITY CLASSIFICATION
Measurement Analysis Corporation 10962 Santa Monica Blvd Los Angeles, California 90025	Unclassified
	2b. GROUP

3. REPORT TITLE

Transducers for Sonic Fatigue Measurement

4. DESCRIPTIVE NOTES *(Type of report and inclusive dates)*

Interim

5. AUTHOR(S) *(Last name, first name, initial)*

Kelly, Ronald D.

6. REPORT DATE	7a. TOTAL NO. OF PAGES	7b. NO. OF REFS
December 1964	107	47

8a. CONTRACT OR GRANT NO. AF 33(615)-1314	9a. ORIGINATOR'S REPORT NUMBER(S)
b. PROJECT NO. 4437	MAC 403-01
c. Task 443706	9b. OTHER REPORT NO(S) *(Any other numbers that may be assigned this report)*
d.	AFFDL-TR-64-171

10. AVAILABILITY/LIMITATION NOTICES

Qualified requesters may obtain copies of this report from DDC. This report has been furnished to OTS for sale to the public

11. SUPPLEMENTARY NOTES	12. SPONSORING MILITARY ACTIVITY
	Air Force Flight Dynamics Laboratory Wright-Patterson AFB, Ohio 45433

13. ABSTRACT

This report discusses the machine errors of transducer systems used for the measurement of dynamic input and response data during sonic fatigue testing. The specific types of transducers covered are accelerometers, microphones, and strain gages. The basic operating principles, intrinsic inaccuracies, environmentally related inaccuracies, and usage inaccuracies are described. These inaccuracies are broken down into errors occuring in the transducer, cabling, and signal conditioner, as well as those due to system operation. In addition, methods for minimizing these errors are given.

DD FORM 1 JAN 64 **1473**

14. KEY WORDS	LINK A		LINK B		LINK C	
	ROLE	WT	ROLE	WT	ROLE	WT
Transducers Instrumentation Sonic Fatigue						

INSTRUCTIONS

1. **ORIGINATING ACTIVITY:** Enter the name and address of the contractor, subcontractor, grantee, Department of Defense activity or other organization (*corporate author*) issuing the report.

2*a*. **REPORT SECURITY CLASSIFICATION:** Enter the overall security classification of the report. Indicate whether "Restricted Data" is included. Marking is to be in accordance with appropriate security regulations.

2*b*. **GROUP:** Automatic downgrading is specified in DoD Directive 5200.10 and Armed Forces Industrial Manual. Enter the group number. Also, when applicable, show that optional markings have been used for Group 3 and Group 4 as authorized.

3. **REPORT TITLE:** Enter the complete report title in all capital letters. Titles in all cases should be unclassified. If a meaningful title cannot be selected without classification, show title classification in all capitals in parenthesis immediately following the title.

4. **DESCRIPTIVE NOTES:** If appropriate, enter the type of report, e.g., interim, progress, summary, annual, or final. Give the inclusive dates when a specific reporting period is covered.

5. **AUTHOR(S):** Enter the name(s) of author(s) as shown on or in the report. Enter last name, first name, middle initial. If military, show rank and branch of service. The name of the principal author is an absolute minimum requirement.

6. **REPORT DATE:** Enter the date of the report as day, month, year; or month, year. If more than one date appears on the report, use date of publication.

7*a*. **TOTAL NUMBER OF PAGES:** The total page count should follow normal pagination procedures, i.e., enter the number of pages containing information.

7*b*. **NUMBER OF REFERENCES:** Enter the total number of references cited in the report.

8*a*. **CONTRACT OR GRANT NUMBER:** If appropriate, enter the applicable number of the contract or grant under which the report was written.

8*b*, 8*c*, & 8*d*. **PROJECT NUMBER:** Enter the appropriate military department identification, such as project number, subproject number, system numbers, task number, etc.

9*a*. **ORIGINATOR'S REPORT NUMBER(S):** Enter the official report number by which the document will be identified and controlled by the originating activity. This number must be unique to this report.

9*b*. **OTHER REPORT NUMBER(S):** If the report has been assigned any other report numbers (*either by the originator or by the sponsor*), also enter this number(s).

10. **AVAILABILITY/LIMITATION NOTICES:** Enter any limitations on further dissemination of the report, other than those imposed by security classification, using standard statements such as:

(1) "Qualified requesters may obtain copies of this report from DDC."

(2) "Foreign announcement and dissemination of this report by DDC is not authorized."

(3) "U. S. Government agencies may obtain copies of this report directly from DDC. Other qualified DDC users shall request through

_____ ."

(4) "U. S. military agencies may obtain copies of this report directly from DDC. Other qualified users shall request through

_____ ."

(5) "All distribution of this report is controlled. Qualified DDC users shall request through

_____ ."

If the report has been furnished to the Office of Technical Services, Department of Commerce, for sale to the public, indicate this fact and enter the price, if known.

11. **SUPPLEMENTARY NOTES:** Use for additional explanatory notes.

12. **SPONSORING MILITARY ACTIVITY:** Enter the name of the departmental project office or laboratory sponsoring (*paying for*) the research and development. Include address.

13. **ABSTRACT:** Enter an abstract giving a brief and factual summary of the document indicative of the report, even though it may also appear elsewhere in the body of the technical report. If additional space is required, a continuation sheet shall be attached.

It is highly desirable that the abstract of classified reports be unclassified. Each paragraph of the abstract shall end with an indication of the military security classification of the information in the paragraph, represented as (*TS*), (*S*), (*C*), or (*U*).

There is no limitation on the length of the abstract. However, the suggested length is from 150 to 225 words.

14. **KEY WORDS:** Key words are technically meaningful terms or short phrases that characterize a report and may be used as index entries for cataloging the report. Key words must be selected so that no security classification is required. Identifiers, such as equipment model designation, trade name, military project code name, geographic location, may be used as key words but will be followed by an indication of technical context. The assignment of links, rules, and weights is optional.